The Journal of Physiology



TOPICAL REVIEW

# Recent advances in the structure, function and regulation of the volume-regulated anion channels and their role in immunity

Sergei Yanushkevich[1], Aleksandra Zieminska[1], Joshua Gonzalez[1], Francisca Añazco[1], Richard Song[1], Alejandra Arias-Cavieres[1], Sara T. Granados[1], Junyi Zou[1], Yan Rao[1] and Axel R. Concepcion[1,2,3,4]

[1]*Department of Biochemistry & Molecular Biology, University of Chicago, Chicago, IL, USA*
[2]*Committee on Immunology, University of Chicago, Chicago, IL, USA*
[3]*Institute for Biophysical Dynamics, University of Chicago, Chicago, IL, USA*
[4]*University of Chicago Medicine Comprehensive Cancer Center, Chicago, IL, USA*

Handling Editors: Laura Bennet & Jorge Contreras

The peer review history is available in the Supporting Information section of this article (https://doi.org/10.1113/JP285200#support-information-section).

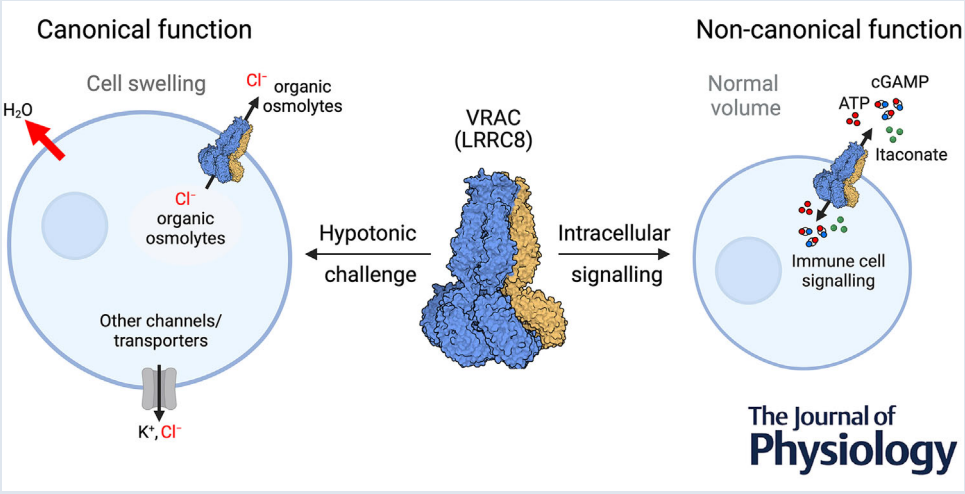


**Abstract figure legend** The volume-regulated anion channel (VRAC), composed of leucine-rich repeat-containing 8 (LRRC8) proteins, serves both canonical and non-canonical functions in vertebrate cells. The canonical function of this channel relates to its original description, which is homeostatic regulation of cell volume in response to hypotonic challenges. In this context, LRRC8-containing VRACs facilitate the regulatory volume decrease process by releasing $Cl^-$ and organic osmolytes. However, most mammalian cells, including immune cells, are not typically exposed to the extreme and prolonged hypotonic conditions that activate VRACs. Emerging evidence suggests that intracellular signalling mechanisms – such as phosphorylation, oxidation and others – may also contribute to the activation of LRRC8-containing VRACs, allowing for the influx of extracellular molecules. Many of these molecules play significant immunomodulatory roles in immune cells. These observations have positioned LRRC8-containing VRACs in the spotlight as a promising target for future immunotherapeutic approaches.

S. Yanushkevich, A. Zieminska and J. Gonzalez contributed equally to this work.



DOI: 10.1113/JP285200

**Abstract** Volume-regulated anion channels (VRACs) are heteromeric complexes formed by proteins of the leucine-rich repeat-containing 8 (LRRC8) family. LRRC8A (also known as SWELL1) is the core subunit required for VRAC function, and it must combine with one or more of the other paralogues (i.e. LRRC8B–E) to form functional heteromeric channels. VRACs were discovered in T lymphocytes over 35 years ago and are found in virtually all vertebrate cells. Initially, these anion channels were characterized for their role in $Cl^-$ efflux during the regulatory volume decrease process triggered when cells are subjected to hypotonic challenges. However, substantial evidence suggests that VRACs also transport small molecules under isotonic conditions. These findings have expanded the research on VRACs to explore their functions beyond volume regulation. In innate immune cells, VRACs promote inflammation by modulating the transport of immunomodulatory cyclic dinucleotides, itaconate and ATP. In adaptive immune cells, VRACs suppress their function by taking up cyclic dinucleotides to activate the STING signalling pathway. In this review, we summarize the current understanding of LRRC8 proteins in immunity and discuss recent progress in their structure, function, regulation and mechanisms for channel activation and gating. Finally, we also examine potential immunotherapeutic applications of VRAC modulation.

(Received 7 October 2024; accepted after revision 20 November 2024; first published online 20 December 2024)
**Corresponding author** A. R. Concepcion: Department of Biochemistry & Molecular Biology, The University of Chicago, 929 East 57th St., GCIS West Bldg, Chicago, IL 60637, USA. Email: aconcepcion@uchicago.edu

## Introduction

Volume regulation is a fundamental process in cell physiology. Cells need to regulate their volume in response to changes that are triggered by osmotic perturbations along with those that occur during their development, proliferation, motility and death (Jentsch, 2016). In vertebrate cells, this is achieved by the transport of $K^+$, $Na^+$ and $Cl^-$ ions, as well as organic osmolytes, through plasma membrane channels and transporters (Kay & Blaustein, 2019; Stein, 1995). The osmotic gradients generated by the movement of these solutes drive water fluxes across the plasma membrane owing to its intrinsic permeability and the presence of aquaporins, ultimately leading to cell volume recovery and homeostasis (Hoffmann et al., 2009). Under hypotonic conditions, mammalian cells activate a coordinated network of channels and transporters to release ions and organic osmolytes, generating an osmotic gradient that favours water efflux and regulatory volume decrease (RVD). Conversely, in situations of hypertonic challenge, cells activate another set of channels and transporters to generate an osmotic gradient that drives water influx and regulatory volume increase (RVI). These homeostatic changes in cell volume are essential to avoid molecular crowding and ionic imbalances that can interfere with cellular signalling and impair cellular functions (Jentsch, 2016).

Volume-regulated anion channels (VRACs) are key components of the ion transport machinery that maintains volume homeostasis in vertebrate cells. Under hypotonic stress, VRACs facilitate the RVD process by releasing $Cl^-$ and small organic osmolytes to the extracellular space. These channels

**Siarhei (Sergei) Yanushkevich** was born in Belarus. He completed his bachelor's degree at Moscow State University, where he received a comprehensive education in biology with a focus on biochemistry. He then pursued a master's degree at Jagiellonian University in Krakow, further honing his skills in protein biochemistry research. Always fascinated by immunology, he joined Axel Concepcion's lab at The University of Chicago, where he applies his expertise in protein biochemistry to the study of T cell-mediated immunity. **Aleksandra Zieminska** obtained her Master's degree in medical biotechnology at the University of Warsaw. Under Dr Concepcion's guidance, she studies the role of LRRC8 channels in T cells in the context of anti-tumour responses. She would like to pursue a PhD to study tumour–immune cell interactions to understand how we can leverage the potential of immune cells in cancer immunotherapy. **Josh Gonzalez** is an undergraduate student at The University of Chicago studying biochemistry and cancer biology as well as working in the Concepcion Lab on structural biology and biophysics. He looks forward to continuing his work on elucidating the structure and mechanical functionality of membrane channels and their role as mediators of immune response.

are composed of paralogues of the leucine-rich repeat-containing 8 (LRRC8) protein family, which assemble in heteromeric complexes. Although most of the studies on LRRC8-containing VRACs have been focused on their role in regulating cell volume, recent findings have shown that these anion channels also participate in the transport of metabolites, second messengers, anticancer drugs and antibiotics under conditions of normal tonicity (Chu et al., 2023; Lahey et al., 2020; Lee et al., 2014; Lutter et al., 2017; Planells-Cases et al., 2015; Wu et al., 2023; Zhou, Chen et al., 2020). These novel, non-canonical functions of VRACs have opened new avenues of research to expand the knowledge of these channels in roles beyond volume regulation. A comprehensive understanding of these roles necessitates precise characterization of their molecular structure and biophysical mechanisms. In this review, we discuss recent advances in the structure–function properties of LRRC8 channels and their role in immune cell function. For a more general overview of the role of LRRC8 channels in a broader context of cell physiology, we refer the readers to excellent reviews that offer extensive information about these channels in cell types and tissues other than immune cells (Chen et al., 2019; Okada, 2024a, 2024b; Osei-Owusu et al., 2018; Strange et al., 2019).

## Historical overview of VRACs in immunity

**Discovery of VRACs in T lymphocytes and other cells in vertebrates.** The initial reports on cell swelling and its connection to increased anion permeability were first documented in Ehrlich ascites cells (Hoffmann, 1978) and human lymphocytes (Grinstein et al., 1983; Grinstein, Clarke, & Rothstein, 1982; Grinstein, Clarke, Dupre et al., 1982). In early 1988, Michael Cahalan and Richard Lewis provided the first electrophysiological evidence of $Cl^-$ currents activated by cell swelling (Cahalan & Lewis, 1988). While attempting to record $Ca^{2+}$ currents in human T cells, a fortunate mistake made by Lewis when adjusting the concentration of ATP in the patch pipette resulted in a hypertonic solution that triggered water influx and T cell swelling (Cahalan & Chandy, 2009). Upon swelling, Cahalan and Lewis noticed a strong outwardly rectifying $Cl^-$ current, and the same current was activated reversibly by exposing T cells to a hypotonic extracellular solution (Cahalan & Chandy, 2009; Cahalan & Lewis, 1988). A few months later, Hazama and Okada reported $Cl^-$ currents with similar properties in human intestine 407 epithelial cells (Hazama & Okada, 1988). Over the next 26 years, the field of VRACs made significant progress in the characterization of both the biophysical properties of these channels and their ability to transport small molecules in different cell types and tissues (Fig. 1) (Jackson & Strange, 1993, 1996; Jackson et al., 1994; Lewis et al., 1993; Manolopoulos et al., 1997; Nilius et al., 1997; Nilius, Oike et al., 1994; Nilius, Sehrer et al., 1994). During this period, several laboratories attempted to identify the genes encoding the VRACs; from these studies, many protein candidates were proposed, but unfortunately, none withstood experimental validations (Strange et al., 2019).

In vertebrate cells, the VRAC currents ($I_{VRAC}$ or $I_{Cl,SWELL}$) are often elicited after a minute, followed by cell swelling in hypotonic solutions, and they are characterized by moderate outward rectification (larger outward currents than inward currents at positive *vs*. negative membrane potentials). In addition, depending on their composition as discussed later, $I_{VRAC}$ inactivates at large positive membrane voltages and has higher permeability to larger halide anions than $Cl^-$. The anion selectivity of VRACs follows an $SCN^- > I^- > NO_3^- > Br^- > Cl^- > F^-$ permeability sequence (Boese et al., 1996) and $I_{VRAC}$ can be completely inhibited by the ethacrynic-acid derivative 4-(2-butyl-6,7-dichlor-2-cyclopentyl-indan-1-on-5-yl) oxybutyric acid (DCPIB) at 10–20 μM concentration (Decher et al., 2001).

**Identification of the LRRC8 gene family.** In 2003, Sawada et al. (2003) identified an atypical cause of

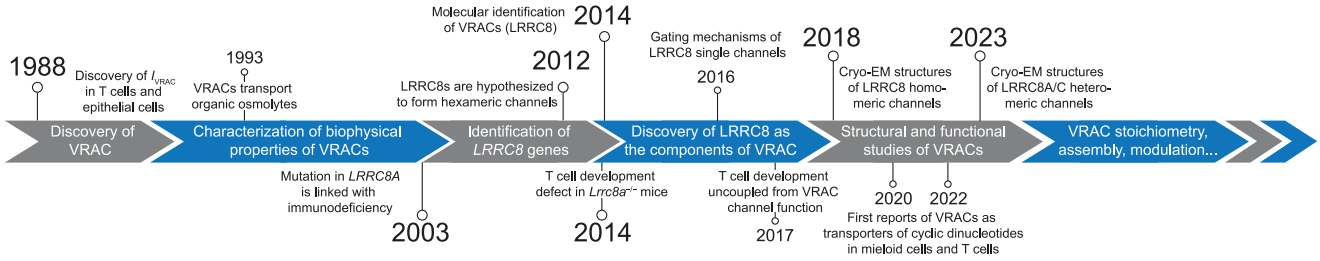


**Figure 1. Timeline of key developments in VRACs**
Since the discovery of VRACs in T lymphocytes and epithelial cells in the late 1980s, research on them has expanded to study their biophysical properties and substrate selectivity. The identification of the LRRC8 proteins as the building blocks of the VRACs in 2014 has revolutionized the field, providing opportunities to research on their structure and function in cell physiology. In the coming years, we expect an increment in the studies on their role in cell physiology, as well as stoichiometry, assembly and modulation of native VRACs.

congenital agammaglobulinaemia in a 17-year-old girl. The karyotypic analysis of the patient showed a t(9;20)(q33.3;q12) translocation, which led to a truncation of the *LRRC8* gene (later identified as *LRRC8A*). The group reported a deletion of 2.5 leucine-rich repeat (LRR) domains and an addition of a 35-intronic amino acid sequence at the C-terminus of the protein (LRRC8A$^{\Delta 91/+35}$). The mutation was thought to be the molecular basis for less than 1% of CD20$^{+}$ B lymphocytes in the peripheral blood of the patient, indicating that the *LRRC8A* gene might be involved in B cell development. Indeed, after introducing the mutated *LRRC8A* gene into murine hematopoietic stem cells and transferring them into lethally irradiated mice, B cell development and differentiation of pro- and pre-B cells were inhibited (Sawada et al., 2003). A year later, the same group identified four additional genes that were structurally similar, highly conserved between humans and mice, and ubiquitously expressed; these genes encoded proteins with multiple LRR domains, and thus they proposed a novel family of LRRC8 proteins (Kubota et al., 2004). The LRR domain is a structural motif characterized by a conserved pattern of hydrophobic leucine residues that form an $\alpha/\beta$ horseshoe fold. Since many proteins with LRR motifs facing the extracellular space were known to mediate protein–protein interactions, adhesion, or function as cell surface receptors, the newly identified LRRC8A proteins were hypothesized to have a ligand involved in B cell development, and thus *LRRC8A* truncation could interfere with receptor–ligand binding (Sawada et al., 2003). In fact, LRR domain-containing proteins are often highly associated with immunity, for example Toll-like receptors, nucleotide-binding oligomerization domain (NOD)-like receptors, or NOD-like receptor pyrin domain containing 3 (NLRP3) inflammasome, in which the LRR motif binds ligands and recognizes molecular patterns, activating innate immune responses (Li & Wu, 2021). Following this idea, Kumar and colleagues generated *Lrrc8a*$^{-/-}$ mice to investigate the role of LRRC8A in lymphocyte development and function. They observed that mice with germline deletion of *Lrrc8a* displayed an aberrant B cell development, but in contrast to previous studies, loss of the full-length LRRC8A protein expression did not interrupt the peripheral B cell fraction, as the cells maintained a normal cell count and functional phenotype. More importantly, knocking out *Lrrc8a* in mice caused a noteworthy block in thymocyte development and impaired peripheral T cell expansion and function, indicating a potential role of LRRC8A in T cell biology (Kumar et al., 2014). It is important to mention that *Lrrc8a*$^{-/-}$ mice showed increased prenatal and postnatal mortality, growth retardation and multiple tissue abnormalities, strongly suggesting a prominent role of LRRC8A in cells and tissues other than lymphocytes. Nevertheless, the authors of this study confirmed the cell-autonomous early block in thymocyte development in the absence of LRRC8A after generating bone marrow chimeric mice (Kumar et al., 2014).

**Discovery of the molecular identity of VRACs… a change in our view (and the topology) of LRRC8 proteins.** Since the discovery of VRACs and the characterization of their biophysical properties, progress in the field was significantly hindered by the lack of knowledge about the molecular identity of the channel (Fig. 1). In 2012, a seminal study published by Abascal & Zardoya proposed that LRRC8 proteins potentially form hexameric channels based on their sequence homology to pannexins (Abascal & Zardoya, 2012). Contrary to what was previously assumed regarding their topological model (Kubota et al., 2004), Abascal and Zardoya hypothesized that LRRC8 proteins assemble in hexameric complexes and extend their LRR domains towards the cytosol, where they could participate in the organization of signalling cascades (Abascal & Zardoya, 2012).

A significant breakthrough occurred in 2014 when two independent groups discovered that VRACs are heteromeric channels formed by LRRC8 proteins (Qiu et al., 2014; Voss et al., 2014). By using genome-wide siRNA screening approaches and high-throughput fluorescence quenching assays of VRAC activity in HEK 293 cells, the laboratories of Ardem Patapoutian and Thomas Jentsch identified that *LRRC8A* expression was essential for VRAC function and RVD (Qiu et al., 2014; Voss et al., 2014). Interestingly, individual deletion of other 'non-essential' LRRC8 paralogues (i.e. LRRC8B–E) did not impact $I_{VRAC}$ activation upon hypotonic cell swelling but rather affected some of its biophysical properties (e.g. current magnitude, rectification and inactivation kinetics at positive membrane potential). However, the presence of the non-essential LRRC8 paralogues in conjunction with LRRC8A expression was necessary to elicit VRAC activation upon hypotonic cell swelling, indicating that LRRC8A by itself is insufficient to trigger strong $I_{VRAC}$ (Voss et al., 2014). These later findings have been validated by multiple research laboratories (Gradogna et al., 2017; Hyzinski-Garcia et al., 2014; Platt et al., 2017; Yamada et al., 2016).

Since the discovery of LRRC8 paralogues as the core components of the VRAC, a significant effort has been made through biochemical studies to uncover key amino acid residues and sequence motifs that are responsible for their plasma membrane expression, electrochemical properties, substrate selectivity and permeability, and potential gating mechanisms. LRRC8 proteins have approximately 800 amino acids, with the initial ∼400 amino acids organized into four transmembrane helices (TM1–TM4). Several amino acid residues within this region are expected to undergo

post-translational modifications, as demonstrated by several high-throughput proteomic studies (Abascal & Zardoya, 2012). Potential phosphorylation residues are concentrated in the loop between TM2 and TM3 (Fig. 2). Additionally, the few identified N-linked glycosylation residues were found in asparagines of the loop between TM1 and TM2 (Voss et al., 2014), and TM3 and TM4 (Fig. 2). This supports the topological model in which both the N- and C-termini face the cytosol, the loop connecting TM2 and TM3 is intracellular (IL1), and the two loops connecting TM1 with TM2 (i.e. EL1) and TM3 with TM4 (i.e. EL2) are extracellular (Fig. 3*A*). This LRRC8 protein topology has been further validated experimentally through immunolabelling and protease protection assays (Lee et al., 2014; Qiu et al., 2014; Voss et al., 2014). The subsequent ∼400 amino acids are unique to LRRC8 proteins and feature 10–17 cytosolic LRRs (Table 1). The LRR domain in each VRAC subunit forms a crescent-shaped structure typical of that observed in many LRR-containing proteins (Deneka et al., 2018). A second intracellular loop (i.e. IL2) links TM4 to the LRR region (Fig. 3*A* and *B*). Abascal and Zardoya proposed that LRRC8 genes originated by tandem duplications, and evolved from the fusion of a pannexin and a LRR motif (Abascal & Zardoya, 2012). Given that pannexin channels lack sensitivity to volume changes, it is anticipated that the LRR domain plays a crucial role in sensing cell swelling and channel gating. Furthermore, the LRR domain is regarded as a versatile domain capable of interacting with various domains in diverse proteins, thereby participating in protein–protein interactions during cell signalling (Kobe & Kajava, 2001).

The discovery of the genes encoding VRACs has led to a renaissance of the field, evidenced by the emergence of the first cryogenic electron microscopy (cryo-EM) structures of LRRC8 channels (Deneka et al., 2018; Kasuya et al., 2018; Kefauver et al., 2018; Kern et al., 2019), as well as an increase in the studies that demonstrate their biophysical properties, regulation and role in cell physiology (Strange et al., 2019). Below, we summarize the current knowledge of the molecular structure of VRACs and highlight key elements crucial for its structure–function relationship.

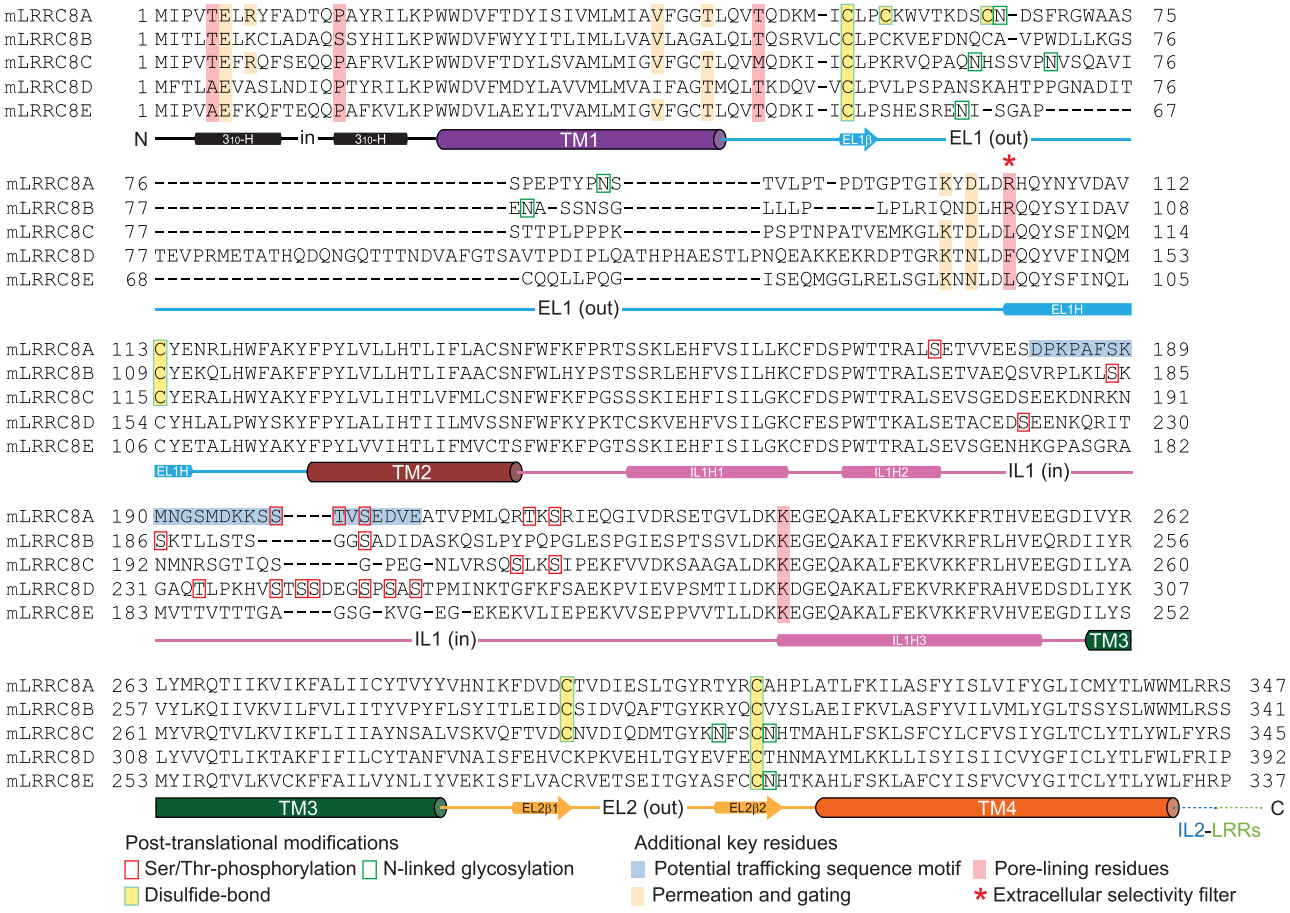


**Figure 2. Alignment of LRRC8 proteins**
Mouse LRRC8 paralogues aligned using Clustal W. The main domains of LRRC8A protein are annotated below. EL, extracellular loop; IL, intracellular loop; LRR, leucine-rich repeat; TM, transmembrane. Key amino acid residues that have been experimentally validated or predicted are boxed (see UniProtKB).

**Table 1. Genomic and proteomic information of human and mouse LRRC8 paralogues**

| | *Homo sapiens* | | | | | *Mus musculus* | | | | |
|---|---|---|---|---|---|---|---|---|---|---|
| Paralogue | Ch | Gene loci | Protein length | Selectivity filter | LRRs[a] | Ch | Gene loci | Protein length | Selectivity filter | LRRs[a] | Additional information[b] |
| LRRC8A | 9 | NC_000009.12 | 810 aa | R103 | 17 | 2 | NC_000068.8 | 810 aa | R103 | 17 | — |
| LRRC8B | 1 | NC_000001.11 | 803 aa | R99 | 13 | 5 | NC_000071.7 | 803 aa | R99 | 15 | Tandem: B-C-D |
| LRRC8C | 1 | NC_000001.11 | 803 aa | L105 | 17 | 5 | NC_000071.7 | 803 aa | L105 | 17 | Tandem: B-C-D |
| LRRC8D | 1 | NC_000001.11 | 858 aa | F143 | 13 | 5 | NC_000071.7 | 859 aa | F144 | 13 | Tandem: B-C-D |
| LRRC8E | 19 | NC_000019.10 | 796 aa | L96 | 11 | 8 | NC_000074.7 | 795 aa | L96 | 10 | — |

[a]Based on UniProt Knowledgebase (UniProtKB); may vary according to cryo-EM data.
[b]Genomic arrangement.

We also discuss various hypotheses regarding VRAC composition and mechanism of action.

## Structural studies of VRACs

The first molecular structures of VRACs were obtained for the homomeric channel of the obligatory subunit LRRC8A (Deneka et al., 2018; Kasuya et al., 2018; Kefauver et al., 2018; Kern et al., 2019). These cryo-EM structures were solved with a resolution of ∼4 Å, revealing that LRRC8A forms hexamers, where six subunits assemble around a central axis of symmetry defining the ion conduction pore (Fig. 4). Subsequently, the structure of the homomeric human LRRC8D channel

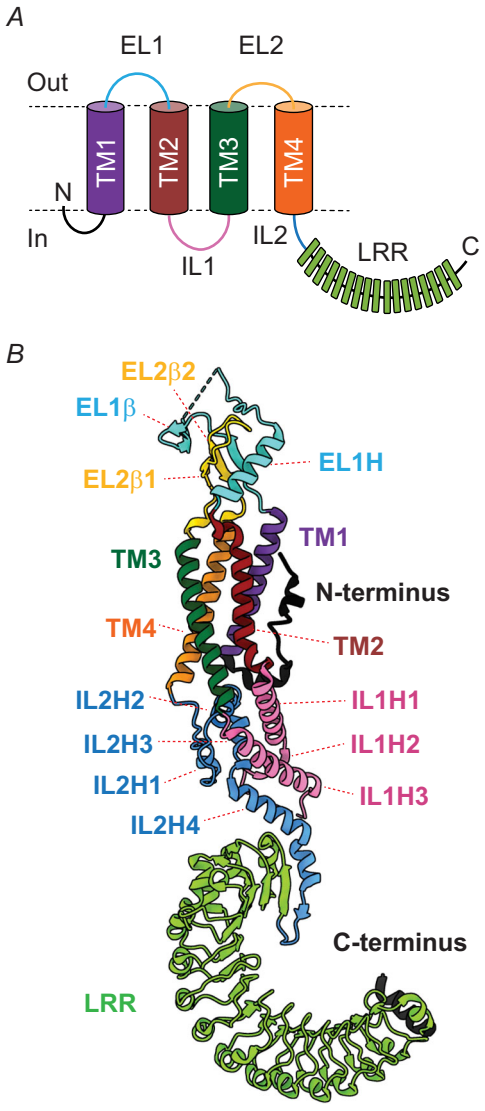


**Figure 3. Membrane topology and folding of LRRC8 proteins**
*A*, membrane topology of LRRC8 proteins. *B*, ribbon representation of the human LRRC8A paralogue in 3D (PDB: 7XZH).

was also published, confirming its hexameric assembly (Nakamura et al., 2020). Unlike these two paralogues, the LRRC8C proteins form heptameric channels with a notably wider pore resembling that of the pannexin channel, which is known to facilitate the transport of larger substrates (Ruan et al., 2020; Rutz et al., 2023). In line with this, LRRC8C chimeric channels possessing 25 amino acids unique to the first intracellular loop of LRRC8A (i.e. LRRC8C-8A$^{IL25}$) that are potentially required for protein trafficking (Yamada & Strange, 2018) also exhibit a heptameric structure (Takahashi et al., 2023). Despite the significance of resolving homomeric LRRC8A, LRRC8C and LRRC8D structures for understanding the fundamental architecture of these channels, there is overwhelming functional data that VRACs, under physiological conditions, form heteromers composed of LRRC8A and at least one other family member, that is, LRRC8B–E (Lahey et al., 2020; Lutter et al., 2017; Qiu et al., 2014; Syeda et al., 2016; Voss et al., 2014). Recently, two independent teams have made important progress by providing the first well-resolved structures of a heteromeric channel composed of LRRC8A and LRRC8C (Kern et al., 2023; Rutz et al., 2023). In Table 2, we summarized the current information regarding 35 experimentally determined cryo-EM structures of LRRC8 complexes from the protein data bank (PDB) archive, which we will discuss in detail in the following sections.

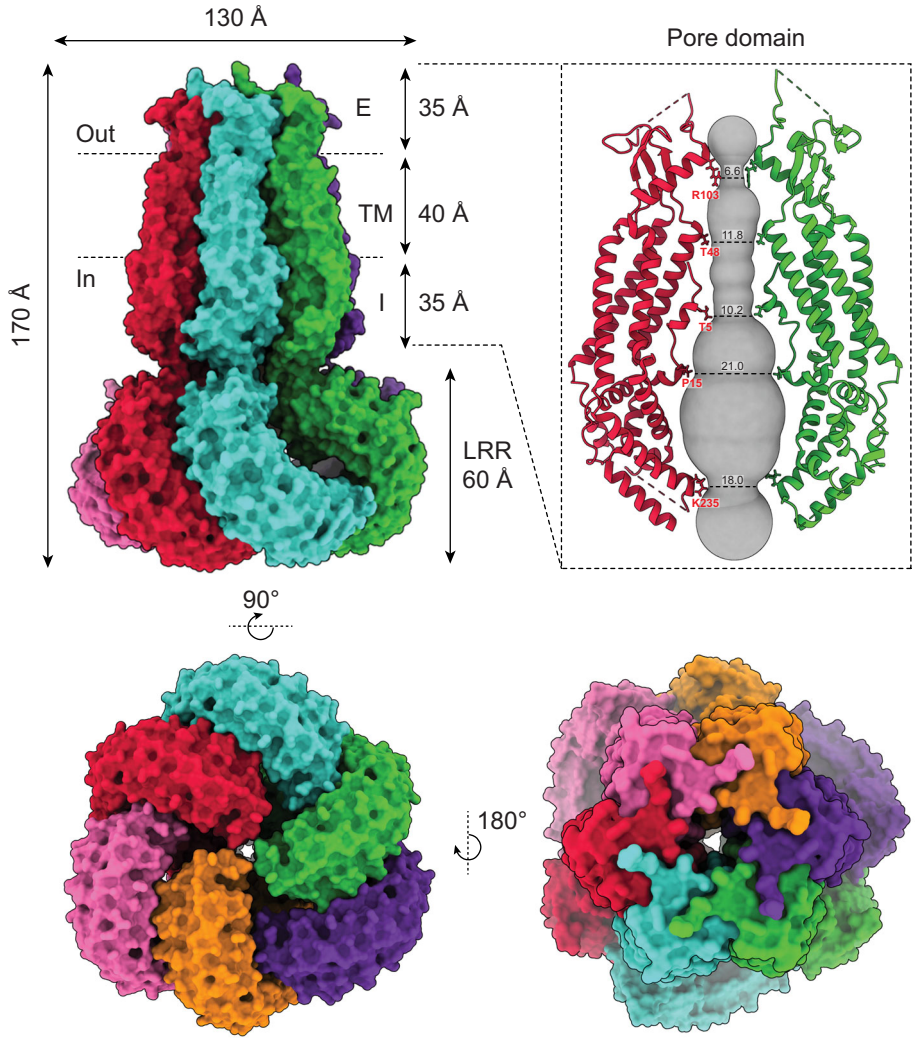


**Figure 4. Architecture of homomeric LRRC8A**
Cryo-EM representation of LRRC8A homohexamer (PDB: 7XZH) viewed from the membrane plane highlighting three subunits, from the cytosolic side (bottom left), and from the extracellular side (bottom right). Each LRRC8A subunit is represented with a different colour. Zoomed-in pore domain of LRRC8A is displayed in relation to two opposite subunits (red in the left and green in the right) with important pore-lining residues is shown in the upper right. The front cyan subunit was removed for clarity. EL, extracellular loop; IL, intracellular loop; LRR, leucine-rich repeat; TM, transmembrane.

**Table 2. Experimentally determined cryo-EM structures of LRRC8 complexes from the protein data bank (PDB) archive**

| LRRC8 complex | Stoichiometry | PDB ID | Species | Expression system | Resolution (Å) | Published pore radius (Å)[a] | Estimated pore radius (Å)[a] | Additional info | References |
|---|---|---|---|---|---|---|---|---|---|
| LRRC8A | 6:0 | 6G8Z | *M. musculus* | HEK293S GnTI- | 3.7 | ∼2.9 Å | 2.72 | Pore domain | Deneka et al. (2018) |
| LRRC8A | 6:0 | 6G9L | *M. musculus* | HEK293S GnTI- | 5.0 | n.r. | 2.60 | | Deneka et al. (2018) |
| LRRC8A | 6:0 | 6G9O | *M. musculus* | HEK293S GnTI- | 4.2 | n.r. | 2.57 | | Deneka et al. (2018) |
| LRRC8A | 6:0 | 6DJB | *H. sapiens* | HEK293-F | 4.4 | ∼0.8* | 0.88 | | Kefauver et al. (2018) |
| LRRC8A | 6:0 | 5ZSU | *H. sapiens* | HEK293S GnTI- | 4.2 | ∼2.1* | 1.90 | | Kasuya et al. (2018) |
| LRRC8A | 6:0 | 6NZW | *M. musculus* | Sf9 | 3.2 | ∼2.0* | 2.05 | Complex with DCPIB, nanodiscs | Kern et al. (2019) |
| LRRC8A | 6:0 | 6NZZ | *M. musculus* | Sf9 | 3.3 | ∼2.1* | 2.37 | Complex with DCPIB, nanodiscs | Kern et al. (2019) |
| LRRC8A | 6:0 | 6O00 | *M. musculus* | Sf9 | 4.2 | n.r. | 1.40 | Apo-LRRC8A in nanodiscs | Kern et al. (2019) |
| LRRC8D | 6:0 | 6M04 | *H. sapiens* | Sf9 | 4.4 | ∼4.0* | 3.95 | N-terminal helix resolved | Nakamura et al. (2020) |
| LRRC8A | 6:0 | 7P5V | *M. musculus* | HEK293S GnTI- | 3.1 | n.r. | 2.80 | Complex with sybody Sb1 (inhibitor) | Deneka et al. (2021) |
| LRRC8A | 6:0 | 7P5W | *M. musculus* | HEK293S GnTI- | 3.5 | n.r. | 0.81 | Complex with sybody Sb2 (inhibitor) | Deneka et al. (2021) |
| LRRC8A | 6:0 | 7P5Y | *M. musculus* | HEK293S GnTI- | 3.3 | n.r. | 2.53 | Complex with sybody Sb3 (weak inhibitor) | Deneka et al. (2021) |
| LRRC8A | 6:0 | 7P60 | *M. musculus* | HEK293S GnTI- | 3.8 | n.r. | 2.33 | Complex with sybody Sb4 (promotor) | Deneka et al. (2021) |
| LRRC8A | 6:0 | 7P6K | *M. musculus* | HEK293S GnTI- | 3.8 | n.r. | 1.76 | Complex with sybody Sb5 (mild promotor) | Deneka et al. (2021) |
| LRRC8A | 6:0 | 7XZH | *H. sapiens* | HEK293S GnTI- | 2.8 | 2.5* | 2.80 | N-terminal helix resolved | Liu et al. (2023) |
| LRRC8A | 6:0 | 7M17 | *M. musculus* | Sf9 | 3.7 | n.r. | 1.76 | Complex with SN-407, nanodiscs | Gunasekar et al. (2022) |
| LRRC8A | 6:0 | 7M19 | *M. musculus* | Sf9 | 3.7 | n.r. | 2.08 | Complex with SN-407, nanodiscs | Gunasekar et al. (2022) |
| LRRC8C | 7:0 | 8B40 | *M. musculus* | HEK293S GnTI- | 4.6 | ∼6.0 | 5.65 | | Rutz et al. (2023) |
| LRRC8A:C | 4:2 | 8B41 | *M. musculus* | HEK293S GnTI- | 3.8 | n.r. | 2.94 | Complex with sybody Sb1 | Rutz et al. (2023) |
| LRRC8A:C | 4:2 | 8B42 | *M. musculus* | HEK293S GnTI- | 6.6 | n.r. | 2.46 | | Rutz et al. (2023) |
| LRRC8A:C | 5:1 | 8DR8 | *M. musculus* | Sf9 | 3.0 | n.r. | 2.55 | BRIL insertion | Kern et al. (2023) |

(*Continued*)

**Table 2. (Continued)**

| LRRC8 complex | Stoichiometry | PDB ID | Species | Expression system | Resolution (Å) | Published pore radius (Å)[a] | Estimated pore radius (Å)[a] | Additional info | References |
|---|---|---|---|---|---|---|---|---|---|
| LRRC8A:C | 5:1 | 8DRE | *M. musculus* | Sf9 | 3.2 | n.r. | 2.54 | BRIL insertion, nanodiscs[b] | Kern et al. (2023) |
| LRRC8A:C | 5:1 | 8DRK | *M. musculus* | Sf9 | 3.0 | n.r. | 2.60 | BRIL insertion | Kern et al. (2023) |
| LRRC8A:C | 5:1 | 8DS3 | *M. musculus* | Sf9 | 3.1 | ∼2.1 | 2.58 | BRIL insertion, nanodiscs[b] | Kern et al. (2023) |
| LRRC8A:C | 5:1 | 8DSA | *M. musculus* | Sf9 | 3.5 | n.r. | 2.32 | BRIL insertion, nanodiscs | Kern et al. (2023) |
| LRRC8A:C | 5:1 | 8DS9 | *M. musculus* | Sf9 | 3.2 | n.r. | 2.31 | BRIL insertion, nanodiscs | Kern et al. (2023) |
| LRRC8A$^{T48D}$:C | 5:1 | 8F7B | *M. musculus* | Sf9 | 3.2 | n.r. | 2.55 | BRIL insertion, nanodiscs | Kern et al. (2023) |
| LRRC8A$^{T48D}$:C | 5:1 | 8F74 | *M. musculus* | Sf9 | 3.1 | n.r. | 2.49 | BRIL insertion, nanodiscs | Kern et al. (2023) |
| LRRC8A$^{T48D}$:C | 5:1 | 8F77 | *M. musculus* | Sf9 | 3.2 | n.r. | 2.49 | BRIL insertion, nanodiscs | Kern et al. (2023) |
| LRRC8A$^{T48D}$:C | 5:1 | 8F79 | *M. musculus* | Sf9 | 3.2 | n.r. | 2.56 | BRIL insertion, nanodiscs | Kern et al. (2023) |
| LRRC8C-8A$^{IL25}$ | 7:0 | 8DXN | *H. sapiens* | Sf9 | 3.4 | ∼4.7 | 4.73 | Chimera in nanodiscs[b] | Takahashi et al. (2023) |
| LRRC8C-8A$^{IL25}$ | 7:0 | 8DXO | *H. sapiens* | Sf9 | 3.6 | ∼4.7 | 4.76 | Chimera in nanodiscs[b] | Takahashi et al. (2023) |
| LRRC8C-8A$^{IL25}$ | 7:0 | 8DXP | *H. sapiens* | Sf9 | 3.7 | ∼4.7 | 4.54 | Chimera in nanodiscs[b] | Takahashi et al. (2023) |
| LRRC8C-8A$^{IL25}$ | 7:0 | 8DXQ | *H. sapiens* | Sf9 | 3.8 | n.r. | 7.13 | Chimera in nanodiscs[c] | Takahashi et al. (2023) |
| LRRC8C-8A$^{IL25}$ | 7:0 | 8DXR | *H. sapiens* | Sf9 | 4.0 | n.r. | 6.84 | Chimera in nanodiscs[c] | Takahashi et al. (2023) |

[a] Extracellular selectivity filter; * Estimated from graph.
[b] Lipid-like densities between subunits and inside pore.
[c] Weak lipid-like densities between subunits and inside pore; n.r. not reported. *H. sapiens*, *Homo sapiens*; *M. musculus*, *Mus musculus*.

**The general structure of VRACs.** The VRAC complex consists of four distinct regions defined as extracellular (E), transmembrane (TM), intracellular (I) and the LRR domain (Fig. 4). The VRAC structure resembles an inverted jellyfish, with its transmembrane and extracellular regions forming six tentacles, while the intracellular and LRR regions create the bell-shaped umbrella. Both the N- and C-termini of the protein are located inside the cell. The channel measures approximately 170 Å in length. The transmembrane spanning region is 40 Å long, while the extracellular region protrudes 35 Å above the cell membrane. The intracellular and LRR regions are 35 and 60 Å long, respectively (Fig. 4) (Liu et al., 2023).

**Pore structure and selectivity filters.** The pore of VRACs is formed by three parts of the protein: a central transmembrane region of approximately 40 Å in length (TM), flanked by two domains extending about 35 Å from the membrane towards both the extracellular (E) and cytoplasmic sides (I). The broad transmembrane region has a cone-shaped form, widening towards the cytoplasm and reaching a diameter of up to 32 Å at the intracellular side of the pore (Fig. 4) (Deneka et al., 2018; Kern et al., 2023; Liu et al., 2023). In contrast, in the part considered to be the selectivity filter of the channel, its extracellular portion narrows to a diameter of 4–14 Å depending on the subunits forming the channel (Figs 4 and 5*A*–*D*) (Deneka et al., 2018; Kern et al., 2019, 2023; Liu et al., 2023; Nakamura et al., 2020; Rutz et al., 2023; Takahashi et al.,

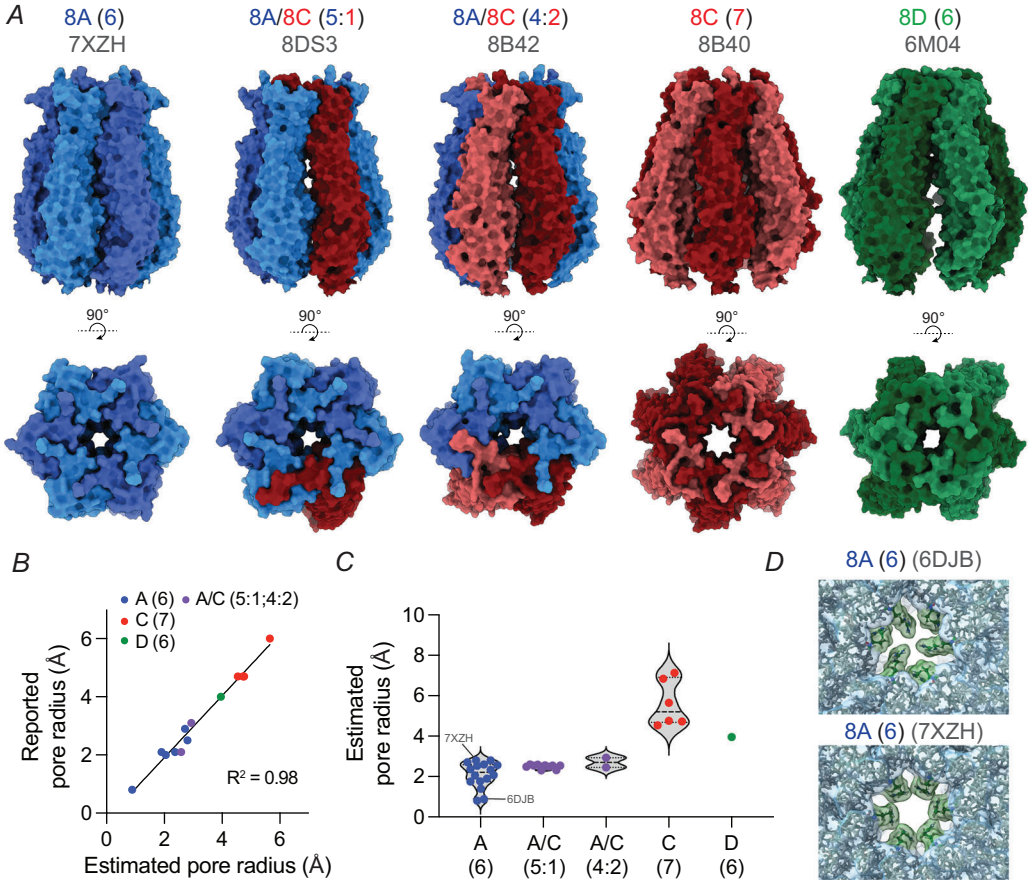


**Figure 5. Pore domain architecture of the homomeric and heterometric LRRC8 complexes**
*A*, cryo-EM representation of LRRC8A homohexamer (PDB: 7XZH), LRRC8A/C 5:1 (PDB: 8DS3) and LRRC8A/C 4:2 (PDB: 8B42) heterohexamers, LRRC8C homoheptamer (PDB: 8B40), and LRRC8D homohexamer (PDB: 6M04) viewed from the membrane plane (top), and from the extracellular side (bottom). *B*, correlation analysis of pore radius at the extracellular selectivity filter in homomeric and heteromeric LRRC8 complexes analysed using HOLE and reported in the literature *versus* our validation of the same structures extracted from PDB and analysed using HOLE pore analysis (see Table 2). *C*, pore radius at the extracellular selectivity filter of all cryo-EM structures of homomeric and heteromeric LRRC8 complexes available in PDB archive and estimated using HOLE pore analysis. *D*, comparison of the pore constriction at the cellular selectivity filter in experimentally determined cryo-EM structures of the homohexameric LRRC8A complex (PDB: 6DJB and PDB: 7XZH) showing the highly dynamic R103 residues and visualized using ChimeraX. The side chain conformation of the R103 altering the pore diameter is shown in green. The pore radii of these two structures are indicated in *C*.

2023). The transmembrane region comprises TM1 and the lower half of TM2 and is characterized by hydrophobic residues facing the pore in the segment that aligns with the hydrophobic core of the membrane bilayer (Takahashi et al., 2023). Additionally, charged amino acid residues are located at both ends, aligning with the phospholipid head groups of the surrounding membrane bilayer (Takahashi et al., 2023). This configuration of the pore-lining surface allows membrane phospholipids to occupy the pore space, effectively sealing it and preventing ion flux through the channel (Kern et al., 2023; Takahashi et al., 2023). In two recent studies by Kern and colleagues and Takahashi and colleagues, lipid-like densities, most likely corresponding to phospholipid molecules, were observed within the channel pore. In the LRRC8A/C heterohexamer structure, these densities were found at the level of the outer leaflet of the lipid bilayer (Kern et al., 2023), while in the LRRC8C-8A$^{IL25}$ chimera (Takahashi et al., 2023), they were observed at both the intracellular and extracellular regions of the transmembrane pore. These observations introduce a completely new perspective on the potential gating mechanism of the VRAC channel, a topic we will explore further below. Interestingly, similar lipid-like densities have been observed in the structures of other large pore channels, such as pannexins and innexins (Burendei et al., 2020; Kuzuya et al., 2022). The role of structural lipid dynamics in the gating of these channels remains to be explored.

The extracellular domain of the VRAC channel comprises two loops, EL1 and EL2. EL1 consists of a $\beta$ strand (EL1$\beta$) followed by an $\alpha$ helix (EL1H). The region between EL1$\beta$ and EL1H is disordered and contains a proline-rich domain (Figs 2 and 3*B*). This region undergoes *N*-glycosylation, which may contribute to protein folding, complex assembly and quality control (Abascal & Zardoya, 2012; Moremen et al., 2012; Voss et al., 2014). EL2 consists of two $\beta$ strands, EL2$\beta$1 and EL2$\beta$2, which interact with EL1$\beta$ to form a three-stranded antiparallel $\beta$ sheet (Figs 2 and 3*B*). The $\alpha$-helix EL1H forms the extracellular part of the pore, where the narrowest region of the ion conduction path is located. Amino acid residues K98 and D100 in LRRC8A and equivalent residues in LRRC8C and LRRC8E, which are located immediately upstream of the EL1H, have been shown to be responsible for the subunit-specific voltage-dependent inactivation kinetics of VRACs (Ullrich et al., 2016). The constriction in EL1H is formed by arginine (R103) in LRRC8A, creating a selectivity filter for anion permeation in heteromeric channels together with positionally equivalent uncharged residues from other LRRC8 paralogues (leucine in LRRC8C and LRRC8E; phenylalanine in LRRC8D; Fig. 2 and Table 1). Experimentally resolved homomeric LRRC8A channels have a constricted electropositive ring with highly dynamic R103 residues at the extracellular selectivity filter (Fig. 5*C* and *D*). The dynamic orientation of these R103 residues changes the pore diameter from ∼2 to ∼6 Å (Deneka et al., 2018; Liu et al., 2023), which may allow the permeation of hydrated chloride anions (∼ 6 Å) when open (Marcus, 1988). However, the LRRC8A homohexamer features a tightly packed and rigid structure and displays small, atypical currents with altered sensitivity to swelling, ionic strength and inhibitors (Liu et al., 2023; Rutz et al., 2023; Yamada et al., 2021). Notably, truncating the bulky R103 by alanine substitutions is insufficient to restore currents in homomeric LRRC8A (Deneka et al., 2018). Conversely, the heteromeric LRRC8A/C(L105R) channel, which has six arginines in its selectivity filter, exhibits similar currents to the wild-type channel. This suggests that the high arginine density at the pore constriction itself does not prevent ion conduction, but rather makes channel highly selective for anions (Deneka et al., 2018). The extracellular pore constriction of homomeric *Hs*LRRC8D is formed by phenylalanine (F143) and has a diameter of 11.5 Å, wider than that of LRRC8A (Nakamura et al., 2020). The pore diameter at the selectivity filter region in the homoheptameric LRRC8C channel, consisting of seven leucines (L105), is further enlarged by 1.3 times compared to the homohexameric *Hs*LRRC8D, reaching the previously estimated pore size of ∼12–14 Å for the native VRAC channel (Fig. 5*B,C*) (Droogmans et al., 1999; Rutz et al., 2023; Takahashi et al., 2023; Ternovsky et al., 2004). Considering that homomeric LRRC8 channels are highly unlikely to appear in physiological conditions as none of the paralogues except LRRC8A alone can target the plasma membrane (Voss et al., 2014), and homomeric LRRC8A exhibits reduced $I_{VRAC}$ function, the incorporation of other subunits would perturb the tightly packed LRRC8A complex. This would increase structural dynamics, determine channel activation properties and expand the range of transported molecules. Indeed, the presence of the LRRC8D subunit in the VRAC channel is sufficient to facilitate the transport of various organic compounds independently of their charge: partially positively charged platinum-based cancer drugs and blasticidin S; neutral *myo*-inositol; zwitterionic taurine, serine and GABA; negatively charged amino acids aspartate and positively charged lysine (Lee et al., 2014; Lutter et al., 2017; Planells-Cases et al., 2015; Schober et al., 2017). At the same time, when the LRRC8E subunit is expressed together with LRRC8A, VRAC selectivity for negatively charged aspartate and glutamate increases (Lutter et al., 2017). Furthermore, heteromeric VRAC channels containing LRRC8E and/or LRRC8C, both of which introduce leucine to the selectivity filter of the VRAC channel, facilitate the transport of negatively charged cyclic dinucleotides such as 2′3′-cyclic GMP–AMP (cGAMP), whereas LRRC8D inhibits their transport (Concepcion et al., 2022; Lahey et al., 2020; Zhou, Chen et al., 2020). The recent cryo-EM structures

of heteromeric LRRC8A/C complexes confirmed that replacing arginine with a smaller hydrophobic leucine in the selectivity ring maintains an expanded filter diameter and makes it less electropositive compared to the homomeric LRRC8A (Fig. 5*C*) (Kern et al., 2023; Rutz et al., 2023). This change may increase conformational flexibility, facilitating the widening of the selectivity filter to transport organic substrates while maintaining the preference for anions. Nevertheless, channels with substitutions replacing R103 of LRRC8A with uncharged residues still maintain selectivity for anions, indicating that other elements along the pore may contribute to anion permeability and selectivity (Deneka et al., 2018; Kasuya et al., 2018; Liu et al., 2023; Yamada & Strange, 2018).

In both connexins and innexins, the N-terminus (NT) forms an $\alpha$-helix that lines the pore and extends in the extracellular direction, thus narrowing the pore and potentially contributing to gating. Mutations in the first 15 amino acids of the LRRC8 NT resulted in alterations in VRAC conductance, ion selectivity and voltage sensitivity (Kefauver et al., 2018; Zhou et al., 2018). While structural studies indicate that the N-termini of LRRC8 proteins do project into the pore, and substituted-cysteine accessibility assays have revealed that several residues of the NT are exposed to the hydrophilic environment, most of the structures obtained for either homomeric LRRC8A or heteromeric LRRC8A/C have undefined N-termini due to the mobility or disorder of this part of the protein. Remarkably, in their study of the homomeric *Hs*LRRC8D protein structure, Nakamura and colleagues were able to observe an N-terminal helix (NTH) entering the channel pore from the cytoplasmic side, resembling what is seen in connexins and innexins (Nakamura et al., 2020). Furthermore, secondary structure predictions of the N-terminal regions of the five LRRC8 isoforms indicate that all LRRC8 isoforms may form NTH (Nakamura et al., 2020), which also aligns with the mutagenesis study by Zhou et al. (2018).

In a recent study (Liu et al., 2023), the complete structure of the NT was resolved for the first time in the homomeric *Hs*LRRC8A. As was observed in *Hs*LRRC8D, connexins, pannexins and innexins, the N-termini of *Hs*LRRC8A fold back towards the pore, constricting the permeation path and determining ion selectivity. However, the NT of LRRC8A adopts a different conformation than the regular $\alpha$-helix seen in other large-pore channels (Fig. 3*B*). The NT of *Hs*LRRC8A comprises amino acid residues M1–L20 and appears as two $3_{10}$-helix conformations (V4–F10 and P15–L20), connected by a loop (A11–Q14) and ending with another loop (M1–P3). The $3_{10}$-helix (P15–L20) proximal to the cytoplasm lies nearly parallel to the bilayer, while the rest of NT lines the pore wall and extends to its extracellular side. These structured NTs participate in both inter- and intra-subunit interactions, stabilizing a tightly packed pore domain at high ionic strength. NT-mediated interactions can be influenced by ionic strength, potentially enabling the N-termini to function as a gating device that alters their interactions with pore-lining transmembrane segments and intracellular loops under reduced ionic strength conditions. This NT potentially forms a second selectivity filter, which, in conjunction with the arginine ring in the extracellular domain, determines the anion permeability of VRACs. This assumption was confirmed using electrophysiology through a series of LRRC8A/C mutants involving key amino acid residues: R103A of LRRC8A and the corresponding L105A of LRRC8C in the extracellular selectivity filter, as well as E6A and R8A in the N-termini of both subunits (Liu et al., 2023). Neutralizing R103 significantly increased the $Na^+$ permeability of the *Hs*LRRC8A/C channel, and the LRRC8A/C (R8A/R8A, R103A/L105A) double mutant exhibited a markedly higher preference for $Na^+$ over $Cl^-$. The E6A mutation not only increased the iodide/chloride permeability ratio ($P_I/P_{Cl}$), but also affected inactivation kinetics (Liu et al., 2023). However, it remains unclear how N-termini may contribute to the regulation of ion conductance in physiologically relevant VRAC heteromers, as no resolved structure of N-termini for the heteromeric channel, nor for intermediate channel activation states showing NTs prior to complete disordering, has been determined to date.

**Organization of intracellular loops and LRR domains.** The cytoplasmic portion of VRAC channels consists of two intracellular loops (IL) and a leucine-rich repeat (LRR) domain. IL1 connects transmembrane helices TM2 and TM3, while IL2 links TM4 with the LRR domain (Fig. 3*A* and *B*). IL1 is composed of three $\alpha$-helices. IL1H2 and IL1H3 are separated by an unstructured region (Fig. 3*B*). The intracellular part of the channel pore is formed by IL1H1 and IL1H3, representing the widest section of the pore (up to 32 Å in diameter in its upper half). It narrows to a constriction of 18 Å on its cytoplasmic side, formed by K235 of the LRRC8A subunit (Fig. 4) (Deneka et al., 2018; Kern et al., 2023; Liu et al., 2023).

The IL1 of LRRC8A has several unique features that set it apart from the rest of the paralogues. First, sequence comparison analysis suggests strikingly high evolutionary conservation of the LRRC8A IL1 compared to IL1 of other paralogues, implying an essential function of this protein region. Second, the intrinsically disordered part of IL1 between IL1H2 and IL1H3, which exhibits the highest sequence variation among paralogues, was predicted to contain molecular recognition elements or features (MoREs/MoRFs) in LRRC8A IL1 using predictor of natural disorder regions (PONDR) analysis (Yamada & Strange, 2018). MoREs/MoRFs are small stretches

of amino acid sequences within intrinsically disordered protein regions that mediate protein–protein interactions. Accordingly, the unique 25-amino-acid sequence in the disordered region of the IL1 in LRRC8A was demonstrated to be sufficient for generating functional homomeric VRACs when inserted into the corresponding region of LRRC8C and LRRC8E (Yamada & Strange, 2018). Furthermore, it is also possible to generate functional homomeric LRRC8D channels by replacing the entire IL1 region with that of LRRC8A (Yamada & Strange, 2018). Hence, this unique region of LRRC8A could play a role in the assembly of LRRC8 subunits into VRACs, trafficking of the channel complex to the plasma membrane and/or in its regulation by cell volume changes.

Yamada and Strange generated several chimeric LRRC8 channels harbouring the key 25 amino acid sequence of LRRC8A IL1, and characterized their electrophysical properties. Thus, they demonstrated that the chimeric LRRC8C-8A($IL^{25}$) channel exhibits sensitivity to cell volume changes and intracellular ionic strength similar to native VRACs, as well as normal DCPIB pharmacology, unlike homohexameric LRRC8A (Yamada et al., 2021). More recently, they resolved the molecular structure of the LRRC8C-8A($IL^{25}$) chimera and showed that it assembles as heptamers (Takahashi et al., 2023). While these chimeric channels exhibit physiological properties like native VRACs and are useful for studying structure–function relationships, it is important to consider that native VRACs are heteromers with potentially variable subunit compositions and stoichiometries.

The second intracellular loop, IL2, links TM4 to the LRR region and consists of four $\alpha$-helices (IL2H1–4, Fig. 3*B*). LRR domains have a horseshoe-shaped conformation and are the most mobile part of the channel (Deneka et al., 2018, 2021; Kasuya et al., 2018; Kefauver et al., 2018; Kern et al., 2019, 2023; Nakamura et al., 2020; Rutz et al., 2023; Takahashi et al., 2023). The fact that LRRC8 channels likely originated from the fusion of pannexin and LRR proteins (Abascal & Zardoya, 2012), and pannexins lack sensitivity to swelling, suggests that the LRR domain plays an essential role in the activation and function of the channel. This notion is further supported by a specific frameshift mutation in mice that truncates the 15 terminal LRRs of LRRC8A. This mutation in *Lrrc8a*, termed *ébouriffé* (*Lrrc8a*$^{ebo/ebo}$), results in a dramatic reduction of VRAC activity in T cells, macrophages and neutrophils (Behe et al., 2017; Platt et al., 2017).

In homomeric LRRC8A in detergent micelles, the LRR domains are organized as a trimer of dimers, forming a stable structure where each LRR domain interacts with both of its adjacent neighbours (Deneka et al., 2018). In contrast, homomeric LRRC8A obtained in lipid nanodiscs exhibits six-fold symmetry (Kern et al., 2019). Furthermore, the homomeric LRRC8D structure has an overall two-fold symmetric dimer of trimers arrangement (Nakamura et al., 2020). Incorporation of LRRC8C to the channel disturbs the arrangement of the LRR domains in LRRC8A, which increases its mobility. In the 5:1 heteromeric structure of LRRC8A:LRRC8C, Kern et al. (2023) were able to distinguish two distinct conformations. In both conformations, the A:C LRR interaction allows for only one additional tight A:A dimer pair. In the first conformation, this pair is separated from the A:C pair by a modified loose A:A interface and a smaller C:A interface. This arrangement results in five stable LRR positions and one flexible LRR of LRRC8A, as there is insufficient space for it to interact with either neighbour. In the second conformation, the LRR domain of LRRC8C directly interacts with the tight A:A dimer, resulting in three stable and three flexible LRRs (Kern et al., 2023). In the 4:2 heteromeric structure of LRRC8A:LRRC8C resolved by Rutz and colleagues, the LRRs of LRRC8A are arranged as two pairs of dimers with tight interaction within each dimer, like the conformation observed in homomeric LRRC8A. However, the two LRRs of LRRC8C do not adopt an A-like conformation and do become more mobile (Rutz et al., 2023). Several pieces of evidence suggest that conformational changes in the VRAC LRR domains are correlated with changes in channel activity. First, when bulky fluorescent proteins are attached to the C-terminus of LRRC8 subunits, the channel demonstrates constitutive activity even in the absence of hypotonic swelling (Gaitan-Penas et al., 2016; Konig et al., 2019). Second, different synthetic nanobodies that bind to distinct epitopes of LRR domains in homomeric LRRC8A either inhibit or enhance the activity of the channel (Deneka et al., 2021). Finally, Förster resonance energy transfer (FRET) measurements combined with patch-clamp experiments, where FRET donor and acceptor fluorescent proteins were attached to the C-termini of different LRRC8 subunits, demonstrated that the rearrangement of LRR domains accompanies channel activation by hypotonic stimulation (Konig et al., 2019). It has been proposed that the LRR motif may function as a mechanosensor in other proteins as well (Ju et al., 2015, 2016). It is noteworthy that the interfaces between interacting LRR motifs contain numerous charged amino acids (Deneka et al., 2018), which could potentially explain how changes in intracellular ionic strength can modulate channel activation (Best & Brown, 2009; Cannon et al., 1998; Emma et al., 1997; Jackson et al., 1996; Nilius et al., 1998; Strange et al., 2019; Syeda et al., 2016).

**Intersubunit gaps in transmembrane region.** Within the transmembrane region, the LRRC8 subunits are less tightly packed, creating gaps on the lipid-facing side of the channel periphery. Depending on the channel

composition, interacting subunits and the hydrophobic environment (detergent *vs.* lipid), these clefts can adopt different shapes and sizes (Deneka et al., 2018; Kern et al., 2019, 2023; Liu et al., 2023; Nakamura et al., 2020; Rutz et al., 2023; Takahashi et al., 2023). For instance, in the most tightly packed homohexameric LRRC8A structure, intersubunit gaps exhibit an 8-shaped configuration with a smaller upper gap and a larger lower gap, separated by a constriction formed by L131 (in TM2) and F324 (in TM4) of neighbouring subunits (Fig. 6*A*) (Deneka et al., 2018; Kern et al., 2019). In the 5:1 heteromeric LRRC8A:LRRC8C structure obtained by Kern and colleagues, the gap in the LRRC8C:LRRC8A interface widens and spreads further into the intracellular region, creating a long polygonal cleft that separates LRRC8C and LRRC8A subunits starting from the extracellular part of the transmembrane region. Meanwhile, gaps between LRRC8A subunits in this heteromeric structure retain the 8-shaped configuration (Fig. 6*B*) (Kern et al., 2023). In the 4:2 heteromeric LRRC8A:LRRC8C channel structure resolved by Rutz and colleagues, the constriction in the middle of the gap between LRRC8A interacting subunits slightly widens, while it completely disappears in the interface between two LRRC8C subunits, resulting in a single prolonged gap in the transmembrane domain (Fig. 6*C*) (Rutz et al., 2023). In the homoheptameric LRRC8C structure of Rutz and colleagues, the protein complex exhibits a seven-fold symmetry, with a single prolonged gap in the transmembrane region between each subunit (Fig. 6*D*). A second gap separates subunits in the intracellular region, which is not visible in either the homomeric LRRC8A or the 4:2 heteromeric LRRC8A:LRRC8C complex. These intersubunit gaps appear different in the homoheptameric structure of the LRRC8C-8A(IL$^{25}$) chimeric channel (Fig. 6*E*). The TM and IC domains are arranged asymmetrically and the subunits are assembled into two groups, one with three subunits and the other with four. The contacts between subunits within each group are tight, resulting in either narrow single gaps or 8-shaped gaps in the TM region (Fig. 6*E*). On the other hand, the two groups of subunits associate via a loose interface, where a wide cleft extends through the entire length of TM and IC domains (Fig. 6*E*) (Takahashi et al., 2023). Finally, in the homomeric LRRC8D structure, the complex exhibits a two-fold symmetry of a dimer of trimers. In the tight interface between subunits within trimers, there is no visible gap, whereas trimers are separated by a long, wide cleft that extends through TM and IC domains, resembling the loose interface in the LRRC8C-8A(IL$^{25}$) chimeric channel (Fig. 6*F*). These differences in the size and shape of intersubunit gaps can illustrate specificities of interaction among different paralogues, which can lead to alterations in complex symmetry and subunit arrangement within heteromeric channels (Kern et al., 2023; Rutz et al., 2023). These alterations could, in turn, impact the activation and function of the VRACs. Furthermore, lipid-like densities were observed within some of these gaps and inside the channel pore, suggesting that phospholipids may seal the gaps (Kern et al., 2019; Liu et al., 2023; Takahashi et al., 2023) and/or participate in gating by moving in and out of the pore through the gaps, similar to what was proposed for the human pannexin1 channel (Kern et al., 2023; Kuzuya et al., 2022).

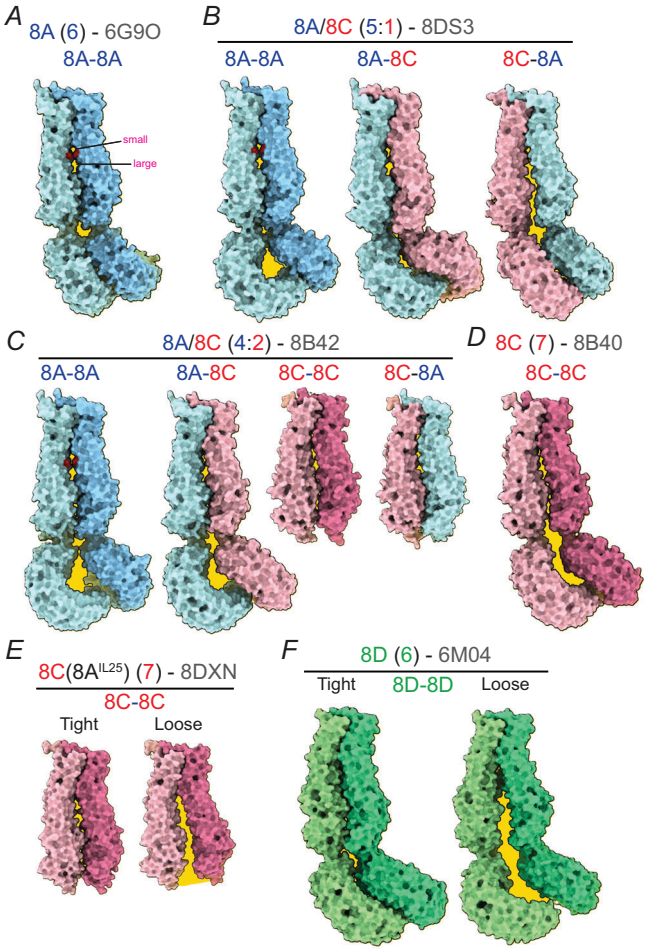


**Figure 6. Intersubunit gaps in homomeric and heteromeric LRRC8 complexes**
Intersubunit gaps (in yellow) between: *A*, LRRC8A subunits in the homohexameric murine LRRC8A channel (PDB: 6G9O); *B*, LRRC8A, and LRRC8A and LRRC8C subunits in the heterohexameric murine LRRC8A/C (5:1) channel (PDB: 8DS3); *C*, LRRC8A, LRRC8A and LRRC8C, and LRRC8C subunits in the heterohexameric murine LRRC8A/C (4:2) channel (PDB: 8B42); *D*, LRRC8C subunits in the homoheptameric murine LRRC8C channel (PDB: 8B40); *E*, LRRC8C subunits in the homoheptameric human LRRC8C-8A$^{IL25}$ chimeric channel (PDB: 8DXN); and *F*, LRRC8D subunits in the homohexameric human LRRC8D channel (PDB: 6M04). Note that some subunits shown in *C* and *E* lack resolved LRR domains.

**The VRAC stoichiometry conundrum.** To date, it is commonly accepted that functional and physiologically relevant VRAC channels are heteromers composed of LRRC8A and at least one other family member, LRRC8B–E (Lahey et al., 2020; Lutter et al., 2017; Planells-Cases et al., 2015; Qiu et al., 2014; Schober et al., 2017; Syeda et al., 2016; Voss et al., 2014). Importantly, the composition of heteromeric channels determines their electrophysiological properties and substrate preferences (Concepcion et al., 2022; Lahey et al., 2020; Lutter et al., 2017; Planells-Cases et al., 2015; Voss et al., 2014; Zhou, Chen et al., 2020). However, it is still unclear whether heteromeric assemblies can encompass all possible combinations of the five different subunits, resulting in an enormous variety of VRAC compositions, or if there are restrictions and regulatory mechanisms at the level of gene expression, subunit synthesis and degradation, channel assembly, and trafficking that reduce the VRAC channel diversity. These mechanisms may enable the formation of distinct channel compositions in different tissues and cell types.

Efforts have been made to determine the number of different subunits present in heteromeric channels produced by cells under physiological conditions or after overexpression of various LRRC8 family members. Gaitán-Peñas and colleagues exploited a stepwise fluorescence photobleaching method to count the number of subunits in LRRC8A:E heteromers expressed in *Xenopus* oocytes (Gaitan-Penas et al., 2016). The average number of LRRC8A and LRRC8E subunits was similar when they were expressed in equimolar levels. Interestingly, the distribution of photobleaching steps fit well with a Poisson distribution but did not follow a binominal distribution, indicating that the number of each particular subunit in heteromers is variable (Gaitan-Penas et al., 2016). Moreover, the channel stoichiometry shifted to a higher LRRC8A content within the complex when three times more LRRC8A complementary RNA was injected relative to LRRC8E. This also led to a decrease in VRAC currents, similar to what was previously observed by Qiu et al. (2014) and Voss et al. (2014), likely by favouring the formation of non-native and non-functional stoichiometries, such as homomeric LRRC8A. Similar results were obtained by Kern and colleagues, who used the same photobleaching approach to count the number of subunits in heteromeric LRRC8A:C channels expressed in HEK 293 cells. The subunit count distribution was similar in cells transfected with a 1:1 ratio of LRRC8A:C and skewed to a higher number of LRRC8A subunits per channel when transfected with 10:1 LRRC8A:C ratio (Kern et al., 2023). These results suggest that the stoichiometry of VRAC channels is not fixed but rather depends on the relative expression levels of different LRRC8 paralogues. Thus, altering the proportion of each subunit could be a potential mechanism for regulating channel activity.

Rutz et al. (2023) examined the distribution of LRRC8A and LRRC8C subunits in endogenous VRACs of HEK 293 cells and in LRRC8A/C channels generated by heterologous overexpression using liquid chromatography with tandem mass spectrometry analysis of purified channels. They found that LRRC8A was the dominant component of VRACs, with an A:C subunit ratio of 1.8:1 in WT cells and 2.9:1 in LRRC8B,D,E 3×KO cells, resulting in four to five copies of LRRC8A subunits in the LRRC8A/C heterohexamers (Rutz et al., 2023). Heterologous overexpression of murine LRRC8A and LRRC8C in LRRC8A-E 5×KO HEK 293 cells yielded an A:C ratio of 2:1 when subunits were transfected in equimolar amounts and slightly shifted to 1.8:1 when LRRC8C DNA was transfected at three times the amount of LRRC8A DNA (Rutz et al., 2023). These results contrast with previous observation by Pervaiz and colleagues that proposed that LRRC8A is a minor component of VRAC heteromers (Pervaiz et al., 2019). The latter group developed and applied a quantitative immunoblot approach to study LRRC8 subunit composition in various mouse cell lines and tissues. The reasons for such discrepancies could lie in differences in the selected cell types and organisms for subunit quantification, unaccounted limitations of the chosen methods, or the assumption that there is a pool of successfully assembled plasma membrane-resident channels where LRRC8A is the dominant subunit. Additionally, there may be additional LRRC8 complexes that are either not properly assembled, in trafficking to the plasma membrane, accumulated in the endoplasmic reticulum (ER) and eventually subjected to ER-associated degradation, or performing some uncharacterized intracellular functions.

Surprisingly, despite the notion that LRRC8 subunits may assemble in variable stoichiometries and potentially interact randomly with each other, Rutz and colleagues found a single distribution where A subunits form a cluster of two tightly interacting pairs, and the two C subunits interact pairwise and are more dynamic. This results in a 4:2 heterohexameric assembly of LRRC8A:C subunits, whereas three distinct assemblies would be expected assuming an unbiased distribution of subunits in channels with an A:C ratio of 2:1 (Rutz et al., 2023). This observation suggests that LRRC8 subunits may indeed have preferences for certain interactions and assembly, and under some expression conditions, this assembly configuration prevails (Fig. 7). Kern and colleagues observed only a 5:1 LRRC8A:C subunit stoichiometry in their structures of heteromeric channels, which may be a specific feature of the insect cell expression system (Kern et al., 2023).

Another interesting question is whether more than two different LRRC8 paralogues can coexist within an individual heteromeric VRAC, or whether an individual cell has multiple channel configurations at the plasma membrane (i.e. LRRC8A:C, LRRC8A:D, etc.). Gaitan-Penas et al. (2016) detected colocalization of LRRC8E–VenusFP and LRRC8D–mCherry on the plasma membrane of *Xenopus* oocytes when untagged 8A subunit and fluorescently labelled 8D and 8E subunits were co-expressed (Gaitan-Penas et al., 2016). In functional assays, Lutter and colleagues demonstrated that the taurine-to-aspartate transport ratio increased when the LRRC8B subunit was added to cells expressing LRRC8A and LRRC8D (Lutter et al., 2017). These changes in substrate selectivity could not be explained by the formation of additional LRRC8A/B channels, as they lack significant transport activity, but rather suggest the formation of VRACs that contain all three subunits in a single heteromeric channel (Lutter et al., 2017). These findings were further supported by sequential co-immunoprecipitations, which confirmed the presence of complexes containing A, C and E subunits (Lutter et al., 2017). However, it has to be taken in consideration that these experiments were performed either in a heterologous expression system or upon DNA transfection in which overexpression of LRRC8 subunits could disrupt the natural generation, assembly, trafficking and degradation of native heteromeric LRRC8 channels.

Finally, it is still an open question whether native VRACs exist only as hexamers or if they can assemble in oligomeric complexes with higher subunit numbers. Native gel, crosslinking and mass spectrometry studies (Syeda et al., 2016), along with photobleaching analyses (Gaitan-Penas et al., 2016), suggest the presence of six to eight LRRC8 subunits per complex. Pannexin channels, which are homologues of LRRC8, have a heptameric structure (Bhat & Sajjad, 2021; Deng et al., 2020; Jin et al., 2020; Kuzuya et al., 2022; Michalski et al., 2020; Mou et al., 2020; Qu et al., 2020; Ruan et al., 2020). Interestingly, homomeric LRRC8C channels with significantly wider pore constriction than any reported hexamers assemble as a heptamer (Rutz et al., 2023; Takahashi et al., 2023). It is possible to hypothesize that channels capable of conducting large organic molecules may indeed have a heptameric structure. However, the fact that LRRC8C requires LRRC8A expression for its trafficking to the plasma membrane strongly suggests that VRACs located at the cell surface are indeed hetero-hexamers and channels with number of subunits higher than six might be a product of overestimation of molecular masses due to glycosylation (Voss et al., 2014) and bound detergent and lipid molecules, which can add up to 20% mass (Wittig et al., 2010). In any case, future single-molecule and structural studies will be crucial in elucidating the stoichiometry and oligomeric state of native LRRC8 heteromers.

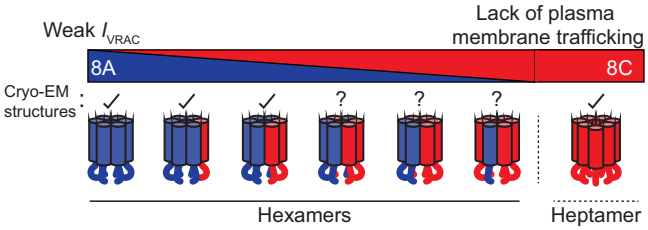


**Figure 7. Hypothetic models of homomeric and heteromeric LRRC8 complexes formed by LRRC8A and LRRC8C paralogues**
Multiple cryo-EM structures of homohexameric LRRC8A and homoheptameric LRRC8C have been resolved by cryo-EM analysis but these channels may lack physiological relevance due to weak $I_{VRAC}$ function upon hypotonic challenge or lack plasma membrane trafficking, respectively. Whether these homomeric channels exist in nature and have physiological functions remains to be determined. Heteromeric LRRC8A/C channels with 5:1 and 4:2 stoichiometries have been resolved by cryo-EM. Heteromeric LRRC8A/C channels with a 3:3, 2:4 or 1:5 configuration have not been found yet.

## VRAC activation and gating

By discussing the structure of VRACs and highlighting key elements of their structure–function relationship, we aim to summarize the evidence and hypothesis regarding VRAC activation and gating. The current canonical role of VRACs is linked to the function they were initially discovered for, which is cell volume regulation in response to hypotonic stress, hence their name. The physical parameters that change due to water influx and cell swelling include: (i) mechanical forces applied to the phospholipid bilayer or underlying cytoskeleton, (ii) reduction in osmolality, and (iii) reduction in intracellular ionic strength. All of these alterations could translate into changes in channel conformation and gating. Initially, researchers focused on understanding how these cues affect VRAC gating. However, most cells in our body do not experience the extreme hypotonic conditions required to activate the VRACs, suggesting the presence of additional physiologically relevant stimuli. Moreover, it is noteworthy that although VRACs facilitate the RVD process, mammalian cells are equipped with additional transporters to balance intracellular osmolality, ionic strength, cell volume and homeostasis (Jentsch, 2016). In strong support of this idea are the findings observed in *Lrrc8a*$^{-/-}$ mice compared to *Lrrc8a*$^{ebo/ebo}$ mutant, in which $Cl^-$ transport induced by hypotonic challenge is impaired (Kumar et al., 2014; Platt et al., 2017). Mice with whole-body deletion of LRRC8A have a striking phenotype characterized by increased prenatal and postnatal mortality, growth retardation and multiple tissue abnormalities (Kumar et al., 2014). In contrast,

*Lrrc8a*$^{ebo/ebo}$ mice that harbour a mutation that truncates the 15 terminal LRRs of LRRC8A – the potential sensor for low ionic strength, as discussed further below – have normal prenatal mortality and growth. These mice also have an increased survival rate compared to *Lrrc8a*$^{-/-}$ mice, with around 60% of the *Lrrc8a*$^{ebo/ebo}$ mice surviving beyond 100 days, while none of the *Lrrc8a*$^{-/-}$ mice survived past that point. Interestingly, *Lrrc8a*$^{ebo/ebo}$ mice share some features with *Lrrc8a*$^{-/-}$ mice, such as curly hair, infertility and kidney abnormalities (Lalouette et al., 1996; Platt et al., 2017). While LRRC8A may have other potential, uncharacterized roles that are not related to channel function, such as acting as a scaffolding protein, it is tempting to speculate that the shared features between *Lrrc8a*$^{-/-}$ mice and *Lrrc8a*$^{ebo/ebo}$ could be linked to the absence of VRAC function in cells that are exposed to osmotic challenges. In contrast, the differences between these two mouse strains may stem from the lack of VRAC complex expression at the cell surface of *Lrrc8a*$^{-/-}$ cells, which would be essential for the influx of extracellular molecules necessary for normal cell physiology. We hypothesize that the absence of LRRC8A expression leads to the removal of VRACs from the cell surface, while the LRRC8A$^{ebo}$ mutant protein may potentially form channel complexes with other LRRC8 paralogues (i.e. LRRC8B-E) and may be activated by cues other than hypotonic stress. Our hypothesis is supported by several observations: (i) the normal expression of LRRC8A$^{ebo}$ mutant protein in T cells from *Lrrc8a*$^{ebo/ebo}$ mice (Platt et al., 2017), (ii) the LRRC8A$^{ebo}$ mutant protein retains the IL1 sequence motif that is crucial for membrane trafficking, and (iii) the LRRC8A$^{ebo}$ mutant maintains intact NT and TM1-4 regions, which are necessary to generate a functional pore domain. Consequently, it is possible that the transport activity of VRACs is preserved in the *Lrrc8a*$^{ebo/ebo}$ mutants compared to *Lrrc8a*$^{-/-}$ mice (Table 3). Nevertheless, this hypothesis requires further testing as it is important to consider that *Lrrc8a*$^{ebo/ebo}$ and *Lrrc8a*$^{-/-}$ mice originate from different genetic backgrounds (BALB/c and FVB/N *vs*. C57BL/6, respectively) (Kumar et al., 2014; Lalouette et al., 1996; Platt et al., 2017). Further supporting this idea, strong evidence highlights the involvement of various signalling pathways in VRAC activation in the absence of hypotonic swelling. These signalling pathways involve reactive oxygen species (ROS) (Gradogna et al., 2017; Shimizu et al., 2004; Varela et al., 2004), phosphorylation events (Bertelli et al., 2021), G-proteins (Voets et al., 1998), ATP (Hyzinski-Garcia et al., 2014; Wang et al., 2024), sphingosine-1-phosphate (Burow et al., 2015; Chu et al., 2023; Kostritskaia et al., 2024; Lahey et al., 2020), cytokines (Zhou, Chen et al., 2020), serum (Chen et al., 2021), and $Ca^{2+}$ and $K^+$ fluxes (Wang et al., 2024). Nevertheless, different groups studying the effects of signal transduction pathways on VRAC activation have obtained contradictory results (Bertelli et al., 2021; Strange et al., 2019). This discrepancy can be potentially explained by the cell- and tissue-specific composition of the heteromeric LRRC8 channel or by other specific factors that mediate signal transduction from a receptor to VRACs.

**Ionic strength and mechanical activation.** A reduction in intracellular ionic strength has been proposed as the primary signal that activates VRACs during cell swelling (Sabirov et al., 2000; Voets et al., 1999). Additionally, LRRC8-containing VRACs were directly activated by low ionic strength in droplet lipid bilayer reconstitution rather than by the increase in droplet volume following fluid injection (Syeda et al., 2016). However, this conclusion is not consistent with similar experimental observations performed in cells. Several studies reported VRAC activation when isotonic fluid was injected into cells or inactivation when negative pressure was applied to the cell membrane, both without altering the intracellular ionic strength (Best & Brown, 2009; Cannon et al., 1998; Poletto Chaves & Varanda, 2008; Zhang & Lieberman, 1996; Zhang et al., 2017). Moreover, the degree of ionic strength reduction required to activate VRACs in the absence of swelling is substantial and unlikely to occur under physiological conditions (Cannon et al., 1998; Nilius et al., 1998; Syeda et al., 2016). This level of reduction is also not achieved during standard whole-cell patch-clamp recordings used to study hypotonic-induced $I_{VRAC}$, where cells are continuously dialysed with a patch pipette solution (Strange et al., 2019). On the other hand, the lack of VRAC activation in lipid droplets following fluid injection does not rule out the potential role of other cellular components, such as the cytoskeleton, in transmitting mechanical tension to the mechanically sensitive module of the LRRC8 protein. Instead, Strange et al. (2019) proposed a model in which mechanical force is the signal that activates VRACs. They postulate that the LRR domains act as channel mechanosensors, with their sensitivity to swelling-induced mechanical force being modulated by ionic strength. In this model, the reduction of ionic strength alters the electrostatic interaction of the LRR domains, thereby reducing the swelling needed to activate VRACs. This model aligns with observations from other groups, where fluorescent proteins linked to the LRR domains cause constitutive VRAC activation (Gaitan-Penas et al., 2016; Konig et al., 2019). Furthermore, FRET measurements between fluorescent proteins attached to C-termini in different LRRC8 subunits, as conducted by König and colleagues, directly demonstrate the connection between LRR domain movements and VRAC gating (Konig et al., 2019). Notably, they could capture the LRRC8 complex at different stages of the secretory pathway and measure the FRET of VRACs located on the ER, Golgi and plasma membrane upon cell swelling. From this,

**Table 3. Genotype-phenotype associations of LRRC8A**

| Genotype | Specie | Model | Protein expression | $I_{VRAC,Cl,Swell}$* or RVD** | Lymphocyte development | Other phenotypes | References |
|---|---|---|---|---|---|---|---|
| LRRC8A$^{WT}$ | *M. musculus*/ *H. sapiens* | 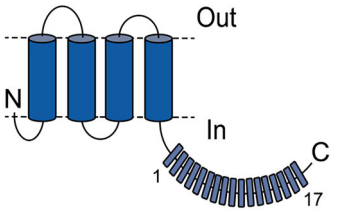  | Yes | Normal | Normal | No | Same as below |
| LRRC8A$^{\Delta 91/+35}$ | *H. sapiens* | 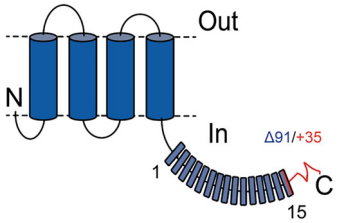  | Yes | Not tested | Impaired (B cells) | Minor facial anomalies | Sawada et al. (2003) |
| LRRC8A$^{ebo}$ | *M. musculus* | 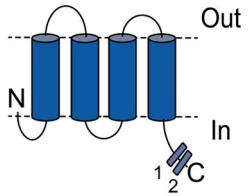  | Yes | Absent* | Normal | Infertility, curly hair, kidney abnormalities, 60% survival at 100 days | Platt et al. (2017) |
| LRRC8A$^{KO}$ | *M. musculus* | N/A | No | Not tested but likely absent | Impaired (T cells, DN2) | Reduced birth and growth, curly hair, all dead at 100 days | Kumar et al. (2014) |
| LRRC8A$^{cKO}$ *Cd4*$^{cre}$ | *M. musculus* | N/A | No | Absent** | Normal | No | Wang et al. (2023) |

*H. sapiens, Homo sapiens; M. musculus, Mus musculus.*

they found that only VRACs that had reached the plasma membrane could respond to hypotonic challenges. In contrast, ER- and Golgi-localized channels did not, despite the homogeneous reduction of ionic strength throughout the cell (Konig et al., 2019). This model aligns with the effects of synthetic nanobodies (sybodies, Sb) binding to the LRR domains on VRAC activation and inhibition (Deneka et al., 2021). Deneka and colleagues showed that nanomolar-affinity binding of sybodies to different regions of the LRR domains can either inhibit VRAC activation under low ionic strength or promote activation even in conditions of elevated ionic strength. This functional effect was clearly illustrated in cryo-EM structures of homomeric LRRC8A complexes with different sybodies. Thus, inhibitory sybodies binding to the convex side of the LRR domain stabilize its structure and reduce its mobility, while potentiating sybodies binding to the loose interface between LRR domains increase their mobility (Deneka et al., 2021). Interestingly, when we analysed the pore domain of homomeric LRRC8A in complex with different sybodies, we found no correlation between the inhibitory or promoting effects of the sybodies on $I_{VRAC}$ activation and the pore radius at the constricting residues along the entire length of the ion-conducting path (Fig. 8*A*) (Deneka et al., 2021). Additionally, we observed a slightly narrower pore radius at the constricted extracellular selectivity filter in homomeric LRRC8A in the complex with Sb4 and Sb5, which are enhancers of $I_{VRAC}$, compared to the complex with inhibitory Sb3 (Fig. 8*A*). These results suggest that the constricted extracellular selectivity filter composed of highly dynamic R103 residues does not prevent ion conduction. Several factors can explain this seemingly counterintuitive observation. Firstly, low ionic strength appears to act as a modulator rather than a direct activator of $I_{VRAC}$. Instead, mechanical forces applied to the LRR domains play a more crucial role (Strange et al., 2019). In this context, the flexibility of the entire VRAC structure and the transmission of conformational changes from the LRR domains to the rest of the channel, especially when induced by mechanical forces, act as the main drivers of VRAC activation. The lack of correlation between constricting residues and the overall VRAC activation could also be explained by the lack of well-resolved N-terminus in these cryo-EM complexes (Fig. 8*A*), which has been suggested to play a crucial role in VRAC gating (Kefauver et al., 2018; Liu et al., 2023; Nakamura et al., 2020; Zhou et al., 2018).

**N-terminus and interpore phospholipids.** Accumulating evidence suggests that the dynamic movement of the intracellular LRR domains is crucial for VRAC activation. However, the physical gate of the channel and the mechanism by which the LRR domains couple with it remain unknown. One potential candidate for the internal gating device is the N-terminal helix, which was recently been found to fold back into the pore of homomeric *Hs*LRRC8A and *Hs*LRRC8D, constricting the permeation path (Fig. 8*B*) and determining ion selectivity, similar to the mechanisms observed in innexins, pannexins and connexins (Liu et al., 2023). However, the lack of resolved structures of the N-terminus in physiologically relevant

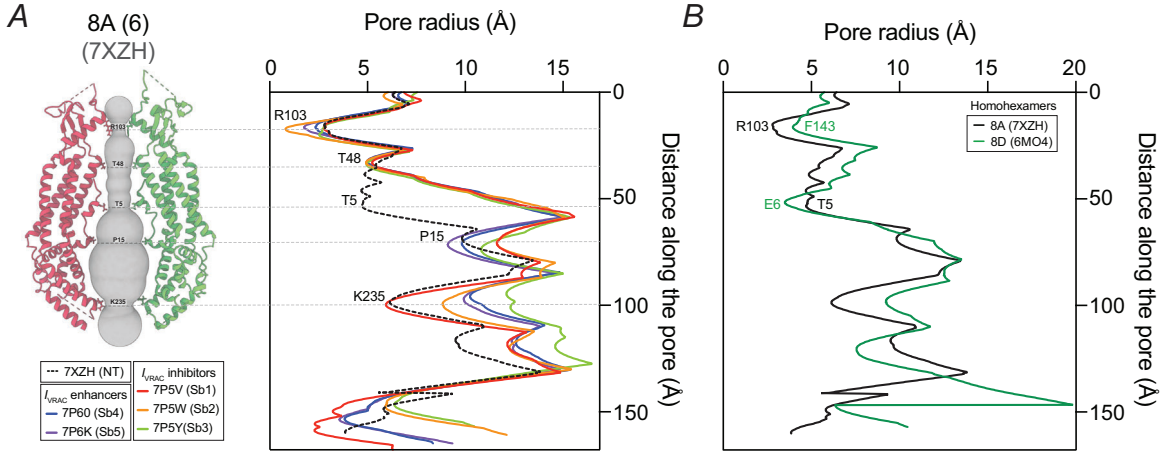


**Figure 8. Pore domain analysis of the homomeric LRRC8 complexes**
*A*, side view of the homomeric LRRC8A pore domain (left; PDB: 7XZH) displayed in relation to two opposite subunits (red in the left and green in the right) with important pore-lining residues, and the pore radius along the symmetry axis (right) in homohexameric LRRC8A channels bound to sybodies (Sb) targeting the LRR domains. Amino acid residues that constrict the pore domain are indicated by the grey dotted lines. PDB codes for LRRC8A homohexamers bound to inhibitory sybodies are as follows: Sb1 (7P5V, red), Sb2 (7P5W, orange) and Sb3 (7P5Y, light green); and enhancer sybodies: Sb4 (7P60, blue) and Sb5 (7P6K, purple). LRRC8A homohexamer with well-resolved N terminus (NT) is shown as a reference (PDB: 7XZH, black dotted lines). *B*, pore radius along the symmetry axis in homohexameric LRRC8A (black; PDB: 7XZH) and LRRC8D (green; PDB: 6MO4) channels with well-resolved NTs.

heteromeric VRACs or during intermediate activation states of the channel limits our understanding of its role in gating.

Another interesting observation was made by two research groups, who revealed lipid densities inside the channel pore in their cryo-EM structures (Kern et al., 2023; Takahashi et al., 2023). Several well-conserved uncharged amino acids among paralogues, namely V40, T44 and T48, are located on the extracellular side of TM1, which extend into the pore. Qiu, Syeda and colleagues demonstrated that mutations of T44 alter channel permeability (Qiu et al., 2014; Syeda et al., 2016). In the heteromeric LRRC8A/C structure resolved by Kern and colleagues, it was shown that V40, T44 and T48 contact pore-bound lipid acyl chains, and their mutations to aspartate disturb TM1–lipid interaction, increasing basal channel activity and substantially reducing hypotonicity-induced activation. Moreover, in the resolved structure of the LRRC8A(T48D):C mutant, there was only weak, discontinuous density at positions occupied by pore lipids in wild-type channels, which is consistent with the idea of a phospholipid-mediated gating mechanism (Kern et al., 2023).

**Oxidation.** ROS should be considered when searching for physiological stimuli unrelated to hypotonic stress and cell swelling. In that regard, Voets et al. (1999) demonstrated that $H_2O_2$ can activate VRACs when applied exogenously or derived from NADPH oxidase under isotonic conditions in HeLa and HCT human cells. Many years later, Gradogna et al. (2017) made an important finding revealing the distinct effect of oxidation on heteromeric VRAC activation depending on its LRRC8 composition. They found that LRRC8A/E heteromers are strongly potentiated by the oxidation of intracellular cysteine residues, independent of hypotonic-induced activation. In contrast, LRRC8A/C and LRRC8A/D heteromers were strongly inhibited by oxidation. Consistent with these findings, endogenous VRAC currents in Jurkat T lymphocytes were similarly inhibited by oxidation, as LRRC8C and LRRC8D paralogues are more strongly expressed than LRRC8E in Jurkat cells (Gradogna et al., 2017). Later, the same group identified specific cysteines in LRRC8E responsible for ROS-mediated VRAC activation (Bertelli et al., 2022). When oxidized, the cysteines C424 and C448 form a disulfide bond between the LRR1 and LRR2 domains in LRRC8E. This promotes a conformational change in the LRRC8A/E complex, leading to channel gating. Interestingly, the group determined that the starting methionine of LRRC8C is a target of oxidation, which inhibits VRAC currents in LRRC8A/C heteromers. Since the same effect was not observed in chimeric proteins where the N-terminus of LRRC8C was replaced with that of LRRC8E, the authors speculated that an oxidized M1 at the N-terminus can occlude the pore when the LRR domains are from LRRC8C but not from LRRC8E proteins. This again suggests that the conformation of the LRR domains plays a crucial role in channel activation.

**Sphingosine-1-phosphate signalling.** Sphingosine-1-phosphate (S1P) is an inflammatory mediator shown to activate VRACs in murine macrophages (Burow & Markwardt, 2014; Burow et al., 2015), microglia (Chu et al., 2023) and human endothelial cells (Lahey et al., 2020). S1P induces VRAC currents through S1P receptors (S1PR1 and S1PR2) and G-protein signalling (Burow & Markwardt, 2014; Burow et al., 2015; Chu et al., 2023; Kostritskaia et al., 2024). Recent research by Kostritskaia et al. (2024) identified the phospholipase C-$\beta$ (PLC-$\beta$) and diacylglycerol (DAG)-dependent protein kinase D (PKD) phosphorylation pathway as a crucial component in the signal transduction process downstream of S1P and G-proteins, necessary for the activation of LRRC8-containing VRACs (Kostritskaia et al., 2024). Moreover, the effect of S1P signalling on VRAC activation was dependent on the actin cytoskeleton in RAW macrophages and on the production of ROS in microglia (Burow et al., 2015; Chu et al., 2023). S1P induces robust ATP release through VRACs in murine macrophages and microglia, which may constitute a functional link between sphingolipid and purinergic signalling during inflammation (Burow et al., 2015; Chu et al., 2023).

**Guanine nucleotide-binding proteins.** The role of guanine nucleotide-binding proteins (or G proteins, for short) in VRAC activation has been extensively investigated by several groups. These proteins belong to a larger group of enzymes called guanosine triphosphatases (GTPases), and their activity is controlled by factors that regulate their ability to bind to and hydrolyse guanosine triphosphate (GTP) to guanosine diphosphate (GDP). The non-hydrolysable GTP analogue GTP$\gamma$S is able to activate VRAC currents in the absence of cell swelling in endothelial and neuroblastoma cells (Estevez et al., 2001; Voets et al., 1998). Conversely, the non-hydrolysable analogue of GDP, GDP$\beta$S, which competes with GTP for nucleotide binding sites on G proteins, caused a time-dependent inhibition of VRACs (Estevez et al., 2001; Voets et al., 1998). This effect was further linked to Rho GTPase signalling and subsequent F-actin cytoskeleton reorganization (Carton et al., 2002; Tilly et al., 1996). However, in other cell types, GTP$\gamma$S and GDP$\beta$S had no visible effect on VRAC activation and inactivation, suggesting a cell type-specific or context-dependent role of these cues (Ackerman et al., 1994; Botchkin & Matthews, 1993).

**Phosphorylation.** Phosphorylation has been extensively studied as a mechanism for VRAC activation. Tyrosine phosphorylation plays a role in VRAC activation during cell swelling as various protein tyrosine kinase (PTK) inhibitors can block VRAC currents when added before a hypotonic stimulus, while protein phosphatase inhibitors (PTP) can potentiate VRACs following a mild hypotonic shock (Bryan-Sisneros et al., 2000; Crepel et al., 1998; Sorota, 1995; Tilly et al., 1993; Voets et al., 1998). Lang and colleagues identified p56lck, a tyrosine kinase from the Src family, as a mediator of swelling-induced chloride channel activation in T lymphocytes (Lepple-Wienhues et al., 1998). However, other studies found no effect of PTK inhibitors on VRACs, and some even observed the opposite results, where PTK inhibitors increased VRAC currents and PTP inhibitors blocked them, even when applied in the same cell line (Du et al., 2004; Ren & Baumgarten, 2005; Thoroed et al., 1999). Further experiments in myocytes revealed an antagonistic mechanism involving two distinct PTK sub-families, with Src kinases exhibiting inhibitory effects and epidermal growth factor receptor kinases showing activating effects (Du et al., 2004; Ren & Baumgarten, 2005). The distinct effects of tyrosine phosphorylation on VRAC activation may result from differences in VRAC composition and stoichiometry across various cell types and tissue-specific regulatory mechanisms of signalling pathways.

Despite some studies showing that DAG-activated protein kinases C (PKCs) are essential for VRAC activation (Hermoso et al., 2004; Hyzinski-Garcia et al., 2014; Roman et al., 1998; Rudkouskaya et al., 2008), other findings have shown either no role for PKCs on VRAC function (Zholos et al., 2005) or even inhibition of VRAC activity (Ben Soussia et al., 2012; Shlyonsky et al., 2011; von Weikersthal et al., 1999), leaving their exact function in VRAC regulation ambiguous. A significant discovery by Konig and colleagues using FRET sensors indicates that PKD plays a crucial role in the hypotonicity-induced activation of VRACs (Konig et al., 2019). PKD acts by converting transient DAG signals into physiological effects downstream of PKC, suggesting that serine/threonine phosphorylation may represent a final regulatory step in VRAC activation (Konig et al., 2019).

**Role of ATP in VRAC activation.** Early studies suggested that intracellular ATP plays a role in swelling-induced VRAC activation, where non-hydrolytic ATP binding to VRACs, rather than phosphorylation, was necessary for this process (Bond et al., 1999; Jackson et al., 1994, 1996). However, the specific ATP binding site remains unidentified, and ATP may be acting indirectly through other regulatory proteins. In line with this idea, a recent significant contribution came from Wang et al. (2024), who revealed a crucial role of extracellular ATP in potentiating cGAMP transport by VRACs in murine macrophages and fibroblasts (Wang et al., 2024). They demonstrated that extracellular ATP binds to the P2X purinergic receptor 7 (P2RX7), triggering $Ca^{2+}$ influx and $K^+$ efflux, which activates VRACs through two mechanisms. First, these ion fluxes induce ROS production, promoting VRAC activation for cGAMP transport. The chelation of cytosolic $Ca^{2+}$ abolished this effect while forcing $Ca^{2+}$ influx with ionomycin resulted in VRAC activation independent of ATP stimulation. Second, they identified the phosphorylation of S174 on the IL1 of LRRC8A subunit as a checkpoint that keeps VRACs closed in a steady state. ATP-induced $K^+$ efflux leads to S174 dephosphorylation, allowing VRAC gating.

## The role of VRACs in immunity

In this section, we summarize the current knowledge on the role of LRRC8 proteins in innate and adaptive immune cells. In the next section, we discuss the therapeutic potential of VRAC modulation in immunity.

**The role of LRRC8 proteins in innate immune cells.** Inflammation is a relevant component of an effective immune response to infection and trauma. However, excessive or chronic inflammation can be harmful and has been implicated in a variety of pathologies, including neurodegeneration, lifestyle diseases and cancer (Furman et al., 2019). Inflammasomes are cytosolic multiprotein complexes responsible for the activation of inflammatory response by innate immune cells. These protein complexes are generated by cytosolic pattern recognition receptors (PRRs) that sense microbe-derived pathogen-associated molecular patterns (PAMPs), damage-associated molecular patterns (DAMPs), or homeostatic disruptions in host cells. Once the inflammasome complex is assembled, it promotes the activation of caspase-1, which in turn cleaves proinflammatory cytokines such as interleukin (IL)-1$\beta$, IL-18 and the pore-forming molecule gasdermin D, resulting in a proinflammatory form of cell death known as pyroptosis and the release of mature proinflammatory cytokines (Zheng et al., 2020). NLRP3 is a critical component of the inflammasome that facilitates the maturation and secretion of proinflammatory cytokines in macrophages (Olona et al., 2022). Early studies have shown that human monocytes treated with PAMPs, such as the bacterial lipopolysaccharide (LPS), under hypotonic conditions induce the release of mature IL-1$\beta$ (Perregaux et al., 1996). Similar results were observed in human and mouse macrophages, suggesting the importance of a volume-regulated response during NLRP3 activation (Compan et al., 2012). More recently, it was shown that NLRP3 activation induced by hypotonic challenge was dependent on

VRACs, as inhibition of these channels with DCPIB or genetic ablation of LRRC8A was sufficient to block hypotonic-induced NLRP3 inflammasome activation in bone-marrow-derived macrophages (BMDMs, Fig. 9*A*) (Green et al., 2020). Intriguingly, this study also found that LRRC8A was dispensable for canonical DAMP-dependent NLRP3 activation (Green et al., 2020). These findings contrast with more recent research that showed the critical role of LRRC8A-containig VRACs in facilitating DAMP-dependent NLRP3 activation triggered by damaged mitochondria, extracellular ATP, and micro-crystals (Chirayath et al., 2024; Wu et al., 2023). In their study, Wu and colleagues provided additional mechanistic insights into the NLRP3 activation regulated by LRRC8-containing VRACs. They demonstrated that LRRC8A modulates NLRP3 inflammasome activation by mediating itaconate efflux and regulating the number of damaged mitochondria (Fig. 9*A*) (Wu et al., 2023). By using conditional knockout mice of LRRC8A in myeloid cells, the authors observed that *Lrrc8a*-deficient BMDMs failed to fully activate canonical NLRP3 upon ATP or nigericin treatment in the presence of LPS (Wu et al., 2023). Interestingly, their electrophysiological studies showed that LRRC8A acts downstream of $K^+$ efflux triggered by ATP- or nigericin-induced NLRP3 activation, as *Lrrc8a*-deficient BMDMs showed normal $K^+$ efflux. To address the mechanism underlying the NLRP3 inhibition in the absence of LRRC8A in macrophages, the authors performed liquid chromatography–mass spectrometry and found, among other mitochondrial metabolites, accumulation of itaconate when macrophages were treated with LPS. Itaconate is an immunomodulatory molecule produced in the mitochondria of activated macrophages through the decarboxylation of *cis*-aconitate, a tricarboxylic acid cycle metabolite. Its role in immunity was first recognized half a century ago when it was identified as an antibacterial agent (McFadden & Purohit, 1977; Rittenhouse & McFadden, 1974; Williams et al., 1971). Itaconate inhibits isocitrate lyase, a key enzyme in the glyoxylate shunt essential during bacterial infection (Li et al., 2023). Since then, numerous studies have shown that itaconate modulates macrophage function, including NLRP3 activation, through various mechanisms (Bambouskova et al., 2021; Hooftman et al., 2020). Whole-cell patch-clamp experiments in which the intracellular $Cl^-$ was replaced with itaconate as the sole permeant anion showed that BMDMs under hypotonic conditions display typical LRRC8A-dependent, DCPIB-sensitive $I_{VRAC}$, strongly suggesting itaconate fluxes through VRACs. Due to lacking VRAC function, *Lrrc8a*-deficient macrophages had increased intracellular accumulation of itaconate and impaired NLRP3 activation (Wu et al., 2023). Lastly, Wu and colleagues went on to show that mice with conditional deletion of *Lrrc8a* in myeloid cells have improved survival in an LPS-induced sepsis model, which correlated with reduced serological and histopathological signs of inflammation (Wu et al., 2023).

VRACs not only promote inflammation by facilitating NLRP3 inflammasome but are also involved in activating and propagating other signalling pathways triggered by PAMP recognition, such as cytosolic DNA (Fig. 9*B*). In mammalian cells, the presence of cytosolic double-stranded DNA (dsDNA) is indicative of cellular damage, infections, or tumorigenesis, and is recognized by a PRR called cyclic GMP-AMP synthase (cGAS) (Sun et al., 2013). When cytosolic dsDNA is detected, cGAS catalyses the synthesis of cGAMP from ATP and GTP. cGAMP is a potent immunomodulatory cyclic dinucleotide (CDN) that binds to the stimulator of interferon genes (STING) protein located in the ER

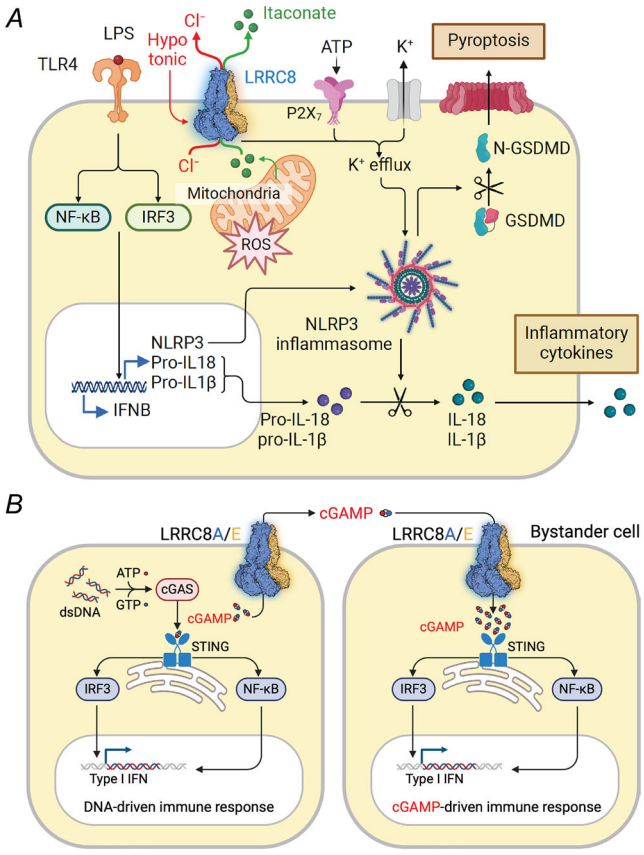


**Figure 9. VRACs induce inflammation in innate immune cells by promoting assembly of the NLRP3 inflammasome and STING-dependent type-I IFN production**
*A*, LRRC8-containing VRACs located in the plasma membrane of macrophages participate in the assembly of the NLRP3 inflammasome by facilitating $Cl^-$ and itaconate efflux upon hypotonic challenge. *B*, LRRC8A/E-containing VRACs mediate the transmission of cGAMP to distant bystander cells. cGAMP produced within the cells that sense double-stranded (ds)DNA or imported through VRACs activates the STING pathway for the production of type-I IFN and host defence. Created with BioRender.com.

(Ablasser et al., 2013). This leads to the association of STING with Tank-binding kinase 1 (TBK1), which then activates interferon regulatory factor 3 (IRF3) and signalling pathways for the production of type-I interferons (IFNs) and host defence. Interestingly, cGAMP activates STING not only in the cells that sense cytosolic dsDNA, but also in nearby cells that lack these danger signals (Ablasser et al., 2013). In 2020, two independent laboratories identified that LRRC8-containing VRACs participate in direct and bi-directional transport of cGAMP (Fig. 9*B*) (Lahey et al., 2020; Zhou, Chen et al., 2020). Zhou and colleagues demonstrated that VRAC blockade with DCPIB or targeted deletion of LRRC8A/E channels resulted in impaired induction of interferon response and increased viral propagation in murine primary macrophages infected with the HSV-1 DNA virus, but not VSV, an RNA virus. Interestingly, IFN response was also compromised in HSV-1-infected LRRC8A/E-deficient murine fibroblasts, underlining the role of VRACs in anti-viral response in both immune and non-immune cells (Zhou, Chen et al., 2020). Whole-cell patch-clamp recordings in human immortalized HeLa cells and HCT116 colon cancer cells showed that the negatively charged cGAMP ($cGAMP^{2-}$) carried a small but significant inward current when intracellular $Cl^-$ was replaced with an equal concentration of $cGAMP^{2-}$, and such currents were blocked by DCPIB or by targeted deletion of LRRC8A, strongly suggesting cGAMP transport through VRACs (Zhou, Chen et al., 2020). Finally, the authors of this study showed that whole-body *Lrrc8e*$^{-/-}$ mice, which were viable and lacked an obvious phenotype, had a severely compromised response to HSV-1 infection, characterized by a reduced type-I IFN response, increased viral load in the lung, liver and kidneys, and an overall increased morbidity and body weight loss compared to wild-type mice. In contrast, *Lrrc8e*$^{-/-}$ mice had normal host defence response to VSV viral infection, strongly suggesting a role of VRACs for host defence against DNA virus *in vivo* (Zhou, Chen et al., 2020). The same year, an independent study by Lahey and colleagues identified that LRRC8 proteins function as ubiquitous cGAMP transporters (Lahey et al., 2020). Using an unbiased CRISPR knockout screen in the human monocyte cell line U937, Lahey et al. (2020) found that LRRC8A was necessary for extracellular cGAMP-mediated STING activation. Interestingly, they made a significant observation that suggests a differential activation of STING signalling depending on the cellular *LRRC8* gene expression, with LRRC8A/C/E positively regulating STING activation upon extracellular cGAMP treatment, LRRC8D negatively regulating STING signalling, and LRRC8B lacking a dominant regulatory role. The effect on STING signalling varied among the different human cell types tested in the study (U937, HEK 293, immortalized endothelial TIME cells, and primary HUVEC endothelial cells), and these differences were attributed to the differential expression of LRRC8 paralogues, strongly suggesting a preference for cGAMP transport based on the VRAC composition (Lahey et al., 2020). Interestingly, the results of cGAMP transport from this study correlate well with the amino acid residues at the pore constriction in the extracellular selectivity filter, in which LRRC8A and LRRC8B display an R103 and R99, respectively; LRRC8C and LRRC8E project a L105 and L96, respectively, and LRRC8D exhibits a F143 (Table 1 and Fig. 2). Despite having a similar amino acid residue at the selectivity filter, the requirement of LRRC8A but not LRRC8B for cGAMP transport can be explained by the obligatory role of LRRC8A expression for channel assembly and trafficking to the plasma membrane (Voss et al., 2014). A relevant finding from these two studies was that STING signalling triggered by cGAMP uptake via VRACs occurs in normotonic conditions and can be further enhanced upon hypotonic challenge (Lahey et al., 2020; Zhou, Chen et al., 2020). This observation raises an outstanding question in the field of VRACs, specifically regarding their potential gating mechanism in normotonic conditions. Recent work in large-pore connexin hemichannels, which are evolutionarily related to LRRC8 proteins (Abascal & Zardoya, 2012), suggests that the permeation of ions and small molecules can be uncoupled and differentially regulated (Gaete et al., 2024). Thus, in contrast to ion permeation, the transport of small molecules is tuned by specific interactions between the permeating molecules and the NT domain that lies within the pore, a general feature of large pore channels (Gaete et al., 2024), including VRACs (Liu et al., 2023; Nakamura et al., 2020). This suggests that cGAMP can be transported along its electrochemical gradient independently of $Cl^-$ fluxes that are triggered by hypotonic cell swelling, potentially through a completely different mechanism and under distinct conditions. However, to mechanistically describe these different modes of actions, more structural studies of VRACs are needed. One potential alternative mechanism could involve the presence of a pervasive molecular cue that modulates VRAC activation. Along these lines, the findings by Wang et al. (2024), which proposed changes in the phosphorylation status of S174 residue in LRRC8A triggered by extracellular ATP to enhance VRAC-mediated cGAMP uptake, become very relevant (Wang et al., 2024). In any case, future work testing these and other hypotheses will be an important step forward to understand the mechanisms of VRAC gating for the uptake of extracellular molecules in normotonic conditions.

Besides their role in promoting inflammation in peripheral and bone marrow-derived macrophages, VRACs have been recently implicated in the release of ATP and neuropathic pain by microglia, the tissue-resident macrophages of the central nervous system (CNS) (Chu et al., 2023). Thus, upon treatment with the inflammatory

lipid mediator S1P in normotonic conditions, the murine BV2 microglial cell line elicited the typical DCPIB-sensitive, outwardly rectifying $I_{VRAC}$ followed by a robust ATP release. *Lrrc8a* deletion in BV2 microglial cells abolished both $I_{VRAC}$ and ATP release upon S1P stimulation, suggesting that LRRC8-containing VRACs may mediate ATP efflux during inflammation in microglial cells (Chu et al., 2023). Electrophysiological studies in HeLa cells demonstrated that LRRC8A mediates $ATP^{4-}$ permeability through VRACs, as both LRRC8A deletion and blockade with DCPIB abolished ATP efflux in these cells. Interestingly, the authors of this work found that conditional ablation of *Lrrc8a* in the mononuclear phagocyte system, including microglia (i.e. with $Lrrc8a^{fl/fl}Cx3cr1^{Cre+}$ mice), alleviates chronic constriction injury (CCI), which is a well-established mouse model of neuropathic pain (Chu et al., 2023). The CCI amelioration in $Lrrc8a^{fl/fl}Cx3cr1^{Cre+}$ mice was supported by a significant reduction of extracellular ATP levels in lumbar spinal cord slices. Moreover, $Lrrc8a^{fl/fl}Cx3cr1^{Cre+}$ mice exhibited decreased spinal microgliosis, dorsal horn neuronal hyperactivity, and both evoked and spontaneous neuropathic pain-like behaviours, indicating a crucial role of LRRC8-containing VRACs in modulating inflammation in the CNS (Chu et al., 2023).

Investigation of LRRC8 proteins in other innate immune cells, including dendritic cells, mast cells, natural killer cells and granulocytes, is currently lacking but is anticipated to progress in the coming years. A study conducted on neutrophils showed that LRRC8A-containing VRACs are present in these cells and are abolished in neutrophils isolated from $Lrrc8a^{ebo/ebo}$ mice, but their ability to kill pathogens in phagosomes was independent of VRAC function (Behe et al., 2017). However, further validation in LRRC8A-KO neutrophils is needed, as $LRRC8A^{ebo}$ mutant channels, even though insensitive to elicit hypotonic-induced $I_{VRAC}$, may still maintain their ability to transport extracellular molecules, possibly explaining the absence of phenotype in these cells (see 'VRAC activation and gating' section for more details).

**The role of LRRC8 proteins in adaptive immune cells.** As discussed in the section 'Historical overview of VRACs in immunity', the discovery of VRACs in T lymphocytes and the identification of the LRRC8 proteins in a patient with a congenital disorder in B cell development strongly suggest that these channels may play a significant role in adaptive immunity. Particularly, in T and B lymphocytes, LRRC8 proteins were initially hypothesized to be surface receptors in which the LRR motif serves as the docking domain for an extracellular ligand that triggers intracellular signalling, activation and function (Kubota et al., 2004; Kumar et al., 2014; Platt et al., 2017). However, the topological model that supports this hypothesis faces significant biophysical challenges. For instance, it is unlikely that a tetraspanin LRRC8 protein that assembles in a heteromeric complex flips its C-terminus towards the extracellular space. Although there are possible mechanisms that might support a change in the membrane topology of LRRC8 proteins, for example, a change in the orientation of the first $\alpha$-helix (TM1) upon insertion of the N-terminus into the ER membrane during the protein biogenesis or alternative splicing that removes one of the TM $\alpha$-helixes of LRRC8 proteins, there is no scientific evidence to support such hypotheses. The current topological model in which LRRC8 proteins extend their N- and C-termini towards the cytosol and assemble with other paralogues is strongly supported by structural data and rules out the possibility of the LRRC8A receptor model. In fact, multiple studies have shown intracellular signalling through the LRR domains in the channel configuration model (Alghanem et al., 2021; Choi et al., 2023; Kumar et al., 2020; Zhang et al., 2017). Therefore, the hypothetical role of LRRC8 proteins as lymphocyte surface receptors will likely fade due to insufficient evidence.

The observation that the cell-intrinsic blockade during early thymic development (i.e. double-negative-2 stage) of $Lrrc8a^{-/-}$ mice is preserved in bone marrow chimeras suggests that LRRC8A may play a role in T cell development. However, this involvement is likely through a mechanism that is independent of volume regulation. A compelling piece of evidence that supports this hypothesis is the normal T cell development observed in both $Lrrc8a^{ebo/ebo}$ mutant mice and $Lrrc8c^{-/-}$ mice, which lack hypotonic-induced $I_{VRAC}$ activation in T cells (Concepcion et al., 2022; Platt et al., 2017). Recent work showed that T-cell-specific conditional knockout mice of *Lrrc8a* (i.e. $Lrrc8a^{fl/fl}Cd4^{Cre+}$) have normal T cell development (Wang et al., 2023). However, an early cell-intrinsic role of LRRC8A in T cell development cannot be ruled out from these mice, as the deletion of the protein occurs later, at the double-positive stage (i.e. $CD4^+CD8^+$ DP thymocytes). In any case, the fact that $Lrrc8a^{ebo/ebo}$ mutant, $Lrrc8a^{fl/fl}Cd4^{Cre+}$ and $Lrrc8c^{-/-}$ mice show normal numbers and proportion of peripheral T cells but lack VRAC function under hypotonic conditions strongly suggests that the volume-regulatory feature of VRACs is dispensable for the maintenance of mature T cells (Concepcion et al., 2022; Platt et al., 2017; Wang et al., 2023).

In mouse and human T cells, VRACs are mainly composed of LRRC8A and LRRC8C paralogues (Concepcion et al., 2022). We identified the selective expression of LRRC8C in T cells using a high-throughput transcriptome profiling screen for ion channels and transporters with increased expression in T cells, compared

to other immune and non-immune cells (Concepcion et al., 2022). We found that the selective expression of LRRC8C in T cells was regulated by the transcription factor signal transducer and activator of transcription 5 (STAT5) upon IL-2 stimulation, a unique feature of the *Lrrc8c* gene compared to the other gene paralogues (Concepcion et al., 2022). Interestingly, due to the lack of redundancy in LRRC8 proteins in these cells, T cells from *Lrrc8c*$^{-/-}$ mice lacked hypotonic-induced $I_{VRAC}$ activation and RVD. Unexpectedly, *Lrrc8c*$^{-/-}$ T cells displayed enhanced proliferation, survival, $Ca^{2+}$ signalling and cytokine production upon TCR stimulation *in vitro*, as well as exacerbated T cell-dependent immune responses *in vivo*, including immunity to influenza A virus infection and experimental autoimmune encephalomyelitis (Concepcion et al., 2022). Because the function of *Lrrc8c*$^{-/-}$ T cells was enhanced even under normotonic conditions, we speculated that the physiological role of VRACs in T cells may be related to the transport of a cargo that suppresses T cell function rather than its role in volume regulation. Thus, we screened various chemical compounds that were previously reported to be transported by VRACs and found the immunomodulatory CDNs to be the only cargo that differentially suppressed the function of wild-type but not *Lrrc8c*$^{-/-}$ T cells (Concepcion et al., 2022). Interestingly, we found a dose response on T cell suppression to the four naturally-occurring CDNs that have been identified so far: the eukaryotic-derived 2′3′-cGAMP, and the bacteria-derived 3′3′-cGAMP, c-di-AMP and c-di-GMP (Concepcion et al., 2022; Danilchanka & Mekalanos, 2013). As discussed in the previous sub-section, CDNs play critical roles in innate immune cells for the activation of the STING pathway, leading to the production of type-I IFN and host defence. However, the activation of STING signalling in T cells induces cell proliferation arrest (Cerboni et al., 2017; Concepcion et al., 2022; Imanishi et al., 2019) and apoptosis (Concepcion et al., 2022; Gulen et al., 2017; Larkin et al., 2017; Wu et al., 2019, 2020). This dual role of STING in activating innate immune cells but inhibiting T cell function is not well understood, and it has been attributed to IFN-independent activities of STING (Wu et al., 2020). In our studies, we found that STING activation by LRRC8C-mediated CDN uptake leads to the accumulation of p53, proliferation arrest, reduced $Ca^{2+}$ influx, apoptosis and overall suppression of T cell function (Fig. 10). It is noteworthy that these changes we observed in *Lrrc8c*$^{-/-}$ T cells occurred exclusively during the stimulation of T cells (Concepcion et al., 2022).

T cell activation is a highly metabolically demanding process that requires significant nutrient uptake for increased protein synthesis (Geltink et al., 2018). T cell activation-associated blasting is thus a result of increased osmolarity inside the cell and subsequent water influx, which leads to overall increased cell size. The major nutrient uptake pathways in T cells are coupled to $Na^+$-cotransport, which, together with other ion channels and transporters, supports the ionic balances that occur during T cell receptor (TCR) stimulation (Feske et al., 2015, 2019; Geltink et al., 2018). Recently, Wang and colleagues showed that the lack of LRRC8A expression in T cells was associated with a slight decrease in TCR signalling and function (Wang et al., 2023), features that seem to be unaltered in *Lrrc8a*$^{ebo/ebo}$ mutant T cells (Platt et al., 2017). They proposed a model in which LRRC8A-containing VRACs prevent excessive volume increase during TCR stimulation while keeping TCR signalling molecules at a density that is optimal for T cell activation and blasting (Wang et al., 2023). However, there was no evidence of such a swollen state of LRRC8A-deficient T cells unless they were subjected to extreme, non-physiological hypotonic challenge (150 mOsm) (Wang et al., 2023). We speculate that the slight decrease in TCR signalling observed in T cells from *Lrrc8a*$^{fl/fl}$*Cd4*$^{Cre+}$ mice might be related to non-volume regulatory features of VRACs because of the following reasons: (i) the normal activation and function of *Lrrc8a*$^{ebo/ebo}$ T cells, which lack hypotonic-induced $I_{VRAC}$ activation (see the section 'VRAC activation and gating' for more details), and (ii) our findings in *Lrrc8c*$^{-/-}$ T cells, which also lack hypotonic-induced $I_{VRAC}$ activation but display enhanced proliferation, survival and cytokine production upon TCR stimulation *in vitro* and *in vivo*

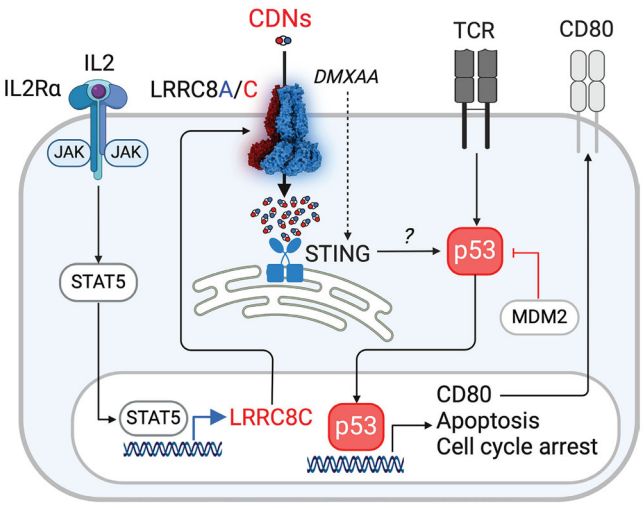


**Figure 10. VRACs suppress T cell function by mediating CDN influx**
LRRC8A/C-containing VRACs located in the plasma membrane of T cells mediate the influx of cyclic dinucleotides (CDNs) to activate the STING pathway. STING activation stabilizes the expression of p53 resulting in cell proliferation arrest, apoptosis, and increased expression of the p53 marker CD80. LRRC8C expression in T cells is modulated by IL-2 receptor and STAT5 signalling. Created with BioRender.com, and modified from Concepcion et al. (2022).

(Concepcion et al., 2022). Further research is needed to clarify these discrepancies.

The studies of LRRC8 proteins in other adaptive immune cells, such as B cells, are limited to the early work that identified the *LRRC8* gene family and later studies in *Lrrc8a*$^{-/-}$ mice (Kumar et al., 2014; Sawada et al., 2003). The congenital agammaglobulinaemia disorder observed in the patient, which is characterized by the lack of peripheral B cells in the blood, together with the defect in B and T cell reconstitution in bone marrow chimeric mice with the LRRC8A$^{\Delta 91/+35}$ mutant, led Sawada et al. (2003) to hypothesize that LRRC8A proteins were required for lymphocyte development. However, as discussed above, there has been a lack of evidence to support this hypothesis over the last 20 years. The fact that *Lrrc8a*$^{-/-}$ mice have modest changes in some B cell subsets but intact intrinsic B cell function (Kumar et al., 2014), as well as no phenotype in B cells reported in *Lrrc8a*$^{ebo/ebo}$ mice, suggests that the defect in lymphocyte development triggered by the LRRC8A$^{\Delta 91/+35}$ mutation may be due to the insertion of the intronic sequence at the C-terminus of LRRC8A rather than a defect in LRRC8A function. The rationale for this hypothesis is that the LRRC8A$^{\Delta 91/+35}$ mutant protein contains almost 90% of the amino acid sequence, including 14.5 intact LRR repeats of the wild-type protein, which may still allow for VRAC function. However, the insertion of a new 35 amino acid intronic sequence at the C-terminus of LRRC8A potentially may cause a VRAC gain-of-function or provide novel, uncharacterized features that are required for lymphocyte development (Table 3).

## Immunotherapeutic outlook of LRRC8 modulation

Given their significant role in regulating immune cell signalling and function, LRRC8-containing VRACs represent a promising target for immunomodulation. In this context, one aspect that is relevant to highlight is the lack of spontaneous phenotypes at the steady state in mice deficient in the *non-essential* subunits of VRACs (i.e. LRRC8B–E). Unlike *Lrrc8a*$^{-/-}$ mice, which exhibit multiple tissue abnormalities (Kumar et al., 2014), whole-body knockout *Lrrc8b*, *Lrrc8c*, *Lrrc8d* and *Lrrc8e* mice survive normally, have normal growth, and show no obvious phenotype (Concepcion et al., 2022; Hayashi et al., 2011; Kumar et al., 2014; Lopez-Cayuqueo et al., 2022; Widmer et al., 2022; Zhou, Chen et al., 2020), except for reported renal injury in *Lrrc8d*$^{-/-}$ mice (Lopez-Cayuqueo et al., 2022). These findings highlight (i) the essential role of LRRC8A for tissue homeostasis, as its expression is necessary for the trafficking of the other paralogues to the plasma membrane, and (ii) the general redundancy of the *non-essential* subunits. Therefore, identifying tissue-specific expression of other paralogues than LRRC8A and understanding the substrate selectivity each paralogue offers in combination with LRRC8A, rather than a general targeting of VRACs, might be an attractive approach for VRAC modulation.

Proof-of-principle experiments using synthetic nanobodies (sybodies) targeting the LRR motifs of LRRC8A have demonstrated allosteric modulation of VRAC function (Deneka et al., 2021). Furthermore, Gunasekar and colleagues have recently shown that small molecule derivatives of the VRAC blocker DCPIB (DCPIB/SN-401) can stabilize LRRC8A expression at the cell surface, subsequently restoring signalling and function in pancreatic $\beta$-cells isolated from mice and humans with type 2 diabetes (Gunasekar et al., 2022). Notably, the DCPIB/N-401 compound has been found to restore glycaemic control, reduce hepatic steatosis/injury, and enhance insulin sensitivity and insulin secretion in a murine model of diabetes *in vivo*, further underscoring the therapeutic potential of VRAC modulation (Gunasekar et al., 2022).

DCPIB is often used in electrophysiology experiments as a potent and selective blocker of VRACs ($IC_{50}$ ~4.1 μM) (Decher et al., 2001). However, it has many undesirable effects, such as interacting with other channels and transporters (Bowens et al., 2013; Deng et al., 2016; Fujii et al., 2015; Lv et al., 2019; Zuccolini et al., 2022), even in cells that lack LRRC8A expression (Afzal et al., 2019). Keeping that in mind, Chu and colleagues conducted a high-throughput fluorescence quenching assay to screen FDA-approved drugs for potential repurposing as VRAC inhibitors. They discovered that dicumarol, a naturally occurring anticoagulant that depletes vitamin K stores, is a novel and potent inhibitor of VRACs ($IC_{50}$ ~4 μM) (Chu et al., 2023). Interestingly, they found that intrathecal administration of dicumarol relieved neuropathic pain-like behaviours in mice, which can be caused by VRAC activation in microglia (Chu et al., 2023). Administering dicumarol to microglia-deficient LRRC8A mice (i.e. *Lrrc8a*$^{fl/fl}$*Cx3cr1*$^{Cre+}$) did not have an additional effect, further supporting the selective and promising role of dicumarol as a clinically available VRAC inhibitor (Chu et al., 2023). More recently, Chen et al. (2024) identified bromadiolone, a second-generation hydroxycoumarin rodenticide from the same family as dicumarol, which also exhibits potent VRAC inhibition ($IC_{50}$ ~1.7 μM) (Chen et al., 2024). Although dicumarol and bromadiolone have strong anticoagulant effects, they could serve as the basis for future medicinal chemistry optimization to enhance their specificity for VRAC channel inhibition (Chen et al., 2024; Chu et al., 2023).

The use of ion channels as targets in immunotherapy is currently a missed opportunity (Feske et al., 2019). However, studies demonstrating their therapeutic potential for immunomodulation are expected to emerge in the next few years (Feske et al., 2019). Future studies

utilizing VRAC modulators in the context of infections, inflammation, autoimmunity and cancer will reveal the therapeutic potential of these channels in immunity. Below, we discuss some ideas in which VRACs may offer immunotherapeutic benefits.

**Modulation of STING signalling by targeting VRACs.** LRRC8-containing VRACs are part of a large network of membrane proteins that transport CDNs, which include the Gap junction components connexin 43 (CX43) and 45 (CX45) (Ablasser et al., 2013), the folate carriers SLC19A1 (Luteijn et al., 2019; Ritchie et al., 2019) and SLC46A2 (Cordova et al., 2021), the ATP-binding cassette transporter ABCC1 (Maltbaek et al., 2022), and the coordinated transport circuit modulated by P2RX7 (Wang et al., 2024; Zhou, Fei et al., 2020). In a recent study, Blest et al. (2024) demonstrated that DNA viruses such as HSV-1 hijack host immune responses by targeting their cGAMP transport machinery, including LRRC8A/C-containing VRACs. The authors of this work identified the HSV-1-derived protein UL56 as a mediator of ubiquitin-dependent degradation of both LRRC8A and LRRC8C, as well as other cGAMP transporters. As a result, HEK 293 cells infected with UL56-expressing HSV-1 showed reduced expression of LRRC8A and LRRC8C proteins, leading to an impaired response to cGAMP treatment and a disrupted STING-mediated antiviral response. On the other hand, HEK 293 cells infected with UL56-deficient HSV-1 were protected from this phenomenon. Although these findings were observed in human cells but not in mouse cells, they provide valuable insights into the evolutionary mechanisms employed by pathogens to evade the host immune response (Blest et al., 2024). Considering these insights, it would be intriguing to investigate whether the DCPIB/N-401 compound can prevent LRRC8A and LRRC8C degradation during HSV-1 infection, thereby facilitating cGAMP transport and STING-mediated antiviral immunity.

The STING pathway plays a critical role in various immune responses. However, the activation of this pathway must be properly balanced as it can have different effects on innate and adaptive immune cells (Lanng et al., 2024; Samson & Ablasser, 2022). The transport of cGAMP through LRRC8 channels observed in macrophages, fibroblasts (Zhou, Chen et al., 2020) and endothelial cells (Lahey et al., 2020) boosts the innate immune response by triggering STING-mediated type-I interferon production. However, excessive STING activation leads to the apoptosis of T and B cells (Concepcion et al., 2022; Gulen et al., 2017; Kuhl et al., 2023; Larkin et al., 2017; Wu et al., 2019, 2020). This opposite effect of STING signalling in different immune cells poses a clinical challenge for immunomodulation. For instance, the STING pathway as a therapeutic approach in anti-tumour immunity has been under active investigation in recent years (Gajewski & Higgs, 2020; Lanng et al., 2024; Samson & Ablasser, 2022). Most of these studies have focused on the direct activation of STING with different agonists that boost *de novo* dendritic cell activation, type-I IFN production and $CD8^+$ T cell cross-presentation to generate tumour-specific $CD8^+$ T cells (Corrales et al., 2015; Deng et al., 2014; Woo et al., 2014). Although preclinical studies in animals showed promising results (Corrales et al., 2015; Deng et al., 2014; Woo et al., 2014), the outcomes in recent clinical trials have been disappointing (Gogoi et al., 2020; Lanng et al., 2024). This unexpected outcome could be in part a consequence of the deleterious effect of STING activation in T cells. Therefore, the modulation of this pathway requires fundamentally new approaches to leverage its use in anti-tumor immunity. In this context, the identification of LRRC8 paralogues in tumour-infiltrating T cells could represent an alternative approach to circumvent the deleterious effect of CDN-induced apoptosis in T cells and enhance antitumour immunotherapy against cancer cells that produce endogenous cGAMP (Carozza et al., 2020; Cordova et al., 2021; Marcus et al., 2018; Wu et al., 2020). The modulation of the STING pathway by targeting LRRC8-containig VRACs is currently limited by the lack of knowledge about the VRAC composition in immune cells (Fig. 11). Future work to uncover the VRAC composition in different immune cell subsets will be a step forward in modulating the STING pathway in immunotherapy.

**Modulation of immune responses by targeting VRAC-mediated itaconate fluxes.** Recent research has revealed that VRACs regulate itaconate efflux in macrophages (Wu et al., 2023). Itaconate is a mitochondrial metabolite with strong immunoregulatory properties and is one of the most abundant metabolites produced by macrophages during inflammation (Strelko et al., 2011; Sugimoto et al., 2012). Itaconate shapes macrophage metabolism and gene expression due to its electrophilic properties, which allow it to modify cysteine residues in various proteins, including enzymes and transcription factors, or to directly inhibit enzyme activity (Li et al., 2023; Qin et al., 2019; Swain et al., 2020). This leads to changes in cytokine production and the inflammatory response of macrophages (He et al., 2022; Swain et al., 2020).

Recent studies have demonstrated the immunomodulatory role of itaconate in T cell differentiation and function. Zhao and colleagues showed that itaconate, secreted by myeloid-derived suppressor cells in the tumour microenvironment, can be taken up by $CD8^+$ T cells, resulting in the suppression of their proliferation, cytokine production and cytolytic activity (Zhao et al.,

2022). Moreover, mice with targeted deletion of *Irg1*, which encodes *cis*-aconitate decarboxylase, the enzyme responsible for producing itaconate, resulted in reduced tumour growth (Zhao et al., 2022). Another study revealed that itaconate can inhibit T helper 17 (Th17) cells and promote regulatory T (Treg) cell differentiation through metabolic and epigenetic reprogramming (Aso et al., 2023). Itaconate decreases *S*-adenosylmethionine levels by inhibiting methionine adenosyl transferase in Th17 cells and reduces 2-hydroxyglutarate by inhibiting isocitrate dehydrogenases (IDH1 and IDH2) in Tregs. This, in turn, alters chromatin accessibility at the *Il17a* and *Foxp3* loci, leading to suppressed IL-17A expression and increased FOXP3 expression. Dysregulation of Th17 and Treg cells is central to the pathology of many autoimmune diseases, including multiple sclerosis, rheumatoid arthritis and lupus erythematosus. Notably, Aso et al. (2023) demonstrated that treating mice with itaconate ameliorated experimental autoimmune encephalomyelitis, suggesting itaconate as a potential treatment for T-cell-mediated autoimmune disorders. Further research is needed to determine the role of VRACs in the modulation of T cell differentiation and function by itaconate. These future studies are expected to emerge in the next few years and will be instrumental in advancing our understanding of the immunomodulatory role of VRACs.

## Concluding remarks

The discovery of the genes encoding VRACs has led to significant expansion in this field over the last 10 years. This research blossoming was possible thanks to the tremendous effort of many scientists who have made solid contributions to characterizing the biophysical properties of these channels and determining their substrate selectivity. Many of the disagreements in the field resulted from the complexity of VRAC composition, which depends on the expression of LRRC8 paralogues in different cell types and tissues.

Currently, there are 35 experimentally determined cryo-EM structures of VRAC complexes in the PDB database. These structures have enhanced our understanding of the molecular organization of the VRAC complex, allowed visualization of the amino acid residues along the pore domain and the extracellular selectivity filter, provided details of the intersubunit gaps in the TM regions, and revealed the arrangements of the LRR domains and intracellular loops. They have also offered invaluable insights into potential VRAC regulatory properties and gating mechanisms. It is expected that additional structures of native channels isolated from primary cells, including immune cells, will emerge in the next few years. Further work on LRRC8 protein biogenesis, post-translational modifications, folding, assembly, trafficking and degradation will be necessary to

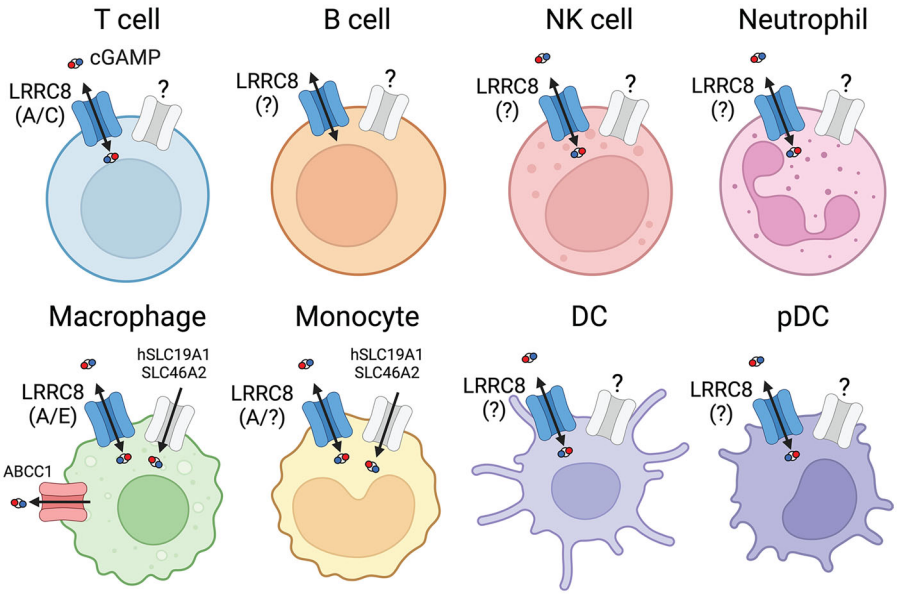


**Figure 11. VRACs and other mechanisms of cGAMP transport in immune cells**
Murine T cells and macrophages transport cGAMP via LRRC8A/C and A/E channels, respectively. Other transporters of cGAMP include the folate carriers SLC46A2 (in human and mouse monocytes and macrophages) and SLC19A1 (in human but not mouse monocytes and macrophages), and the ABCC1 transporters (in murine macrophages). The mechanisms of cGAMP transport in B and NK cells, neutrophils, dendritic cells (DCs) and plasmacytoid dendritic cells (pDCs) are still unknown. Created with BioRender.com.

better understand how these channels are built and how they regulate cell physiology.

Based on the biochemical, structural and functional studies discussed here, we conclude that LRRC8A protein has unique features that make it the essential component of the channel: (i) LRRC8A possesses the sequence motif for potential trafficking to the cell surface, which means that other LRRC8 paralogues need to interact with LRRC8A for membrane trafficking, assembly and the generation of functional heteromeric channels at the cell surface. This requirement may prevent the generation of large-pore channels (e.g. heptameric LRRC8C) that potentially have weaker control checks for plasma membrane anion permeation. (ii) LRRC8A controls VRAC permeation by locking the channel and controlling its gating. The tight homomeric LRRC8A assemblies very likely explain the poor anion conductivity of these channels when exposed to hypotonic challenge. Interestingly, mechanical forces applied to the LRR domains with sybodies that bind between their loose interface can provoke allosteric changes that translate into potentiation of anion conductivity in homomeric LRRC8A channels. These allosteric mechanisms cause conformational changes along the pore domain but with low impact at the extracellular selectivity filter, suggesting that VRACs have a gate that seals the channel from the inside, potentially involving the N-termini pointing towards the pore axis. Therefore, the combination of LRRC8A with other paralogues seems to provide flexibility to the channel assembly and allows anion efflux for volume regulation when cells are exposed to a hypotonic challenge. (iii) Combining LRRC8A with other paralogues also diversifies the substrate selectivity of VRACs to uptake extracellular molecules that can potentially permeate these channels following a concentration gradient. Additional cues triggered by intracellular signalling (e.g. phosphorylation, oxidation, etc.) may operate VRAC gating to enhance the influx of extracellular molecules. This dual gating path model offers a molecular explanation for the shared and distinct phenotypes observed in mutant mice that lack VRAC channels at the cell surface (i.e. LRRC8A$^{-/-}$) or lack cellular response to hypotonic challenge but preserve plasma membrane expression of VRACs (i.e. LRRC8A$^{ebo}$).

Finally, coming back to the evolutionary origins of VRACs, it is possible that these channels emerged to equip vertebrate cells with various capabilities to better adapt to diverse environments, including hypotonic challenges. However, most cells in our body, like immune cells, rarely experience such extreme conditions that would activate these channels. Therefore, it is not unreasonable to speculate that VRACs also equipped vertebrate immune systems to respond more efficiently to pathogens by enhancing CDN uptake, among other functions. In this context, the emergence of VRACs aligns with the ability of the STING protein to trigger type-I IFN via the IRF3 transcription factor (Margolis et al., 2017), which is the primary antiviral output in mammals. Furthermore, the large cargo transported by VRACs that has been reported thus far could represent just a fraction, and it is possible that additional substrates not yet identified can be taken up by these channels to modulate cell signalling and function under normotonic conditions. Future studies on channel gating mechanisms will uncover the true fundamental role of VRACs in cell physiology and could significantly influence our understanding of these channels in cell function and disease.

## References


Abascal, F., & Zardoya, R. (2012). LRRC8 proteins share a common ancestor with pannexins, and may form hexameric channels involved in cell-cell communication. *BioEssays*, **34**(7), 551–560.

Ablasser, A., Schmid-Burgk, J. L., Hemmerling, I., Horvath, G. L., Schmidt, T., Latz, E., & Hornung, V. (2013). Cell intrinsic immunity spreads to bystander cells via the intercellular transfer of cGAMP. *Nature*, **503**(7477), 530–534.

Ackerman, M. J., Wickman, K. D., & Clapham, D. E. (1994). Hypotonicity activates a native chloride current in *Xenopus* oocytes. *Journal of General Physiology*, **103**(2), 153–179.

Afzal, A., Figueroa, E. E., Kharade, S. V., Bittman, K., Matlock, B. K., Flaherty, D. K., & Denton, J. S. (2019). The LRRC8 volume-regulated anion channel inhibitor, DCPIB, inhibits mitochondrial respiration independently of the channel. *Physiological Reports*, **7**(23), e14303.

Alghanem, A. F., Abello, J., Maurer, J. M., Kumar, A., Ta, C. M., Gunasekar, S. K., Fatima, U., Kang, C., Xie, L., Adeola, O., Riker, M., Elliot-Hudson, M., Minerath, R. A., Grueter, C. E., Mullins, R. F., Stratman, A. N., & Sah, R. (2021). The SWELL1-LRRC8 complex regulates endothelial AKT-eNOS signaling and vascular function. *eLife*, **10**, e61313.

Aso, K., Kono, M., Kanda, M., Kudo, Y., Sakiyama, K., Hisada, R., Karino, K., Ueda, Y., Nakazawa, D., Fujieda, Y., Kato, M., Amengual, O., & Atsumi, T. (2023). Itaconate ameliorates autoimmunity by modulating T cell imbalance via metabolic and epigenetic reprogramming. *Nature Communications*, **14**(1), 984.

Bambouskova, M., Potuckova, L., Paulenda, T., Kerndl, M., Mogilenko, D. A., Lizotte, K., Swain, A., Hayes, S., Sheldon, R. D., Kim, H., Kapadnis, U., Ellis, A. E., Isaguirre, C., Burdess, S., Laha, A., Amarasinghe, G. K., Chubukov, V., Roddy, T. P., Diamond, M. S., Jones, R. G., Simons, D. M., & Artyomov, M. N. (2021). Itaconate confers tolerance to late NLRP3 inflammasome activation. *Cell Reports*, **34**(10), 108756.

Behe, P., Foote, J. R., Levine, A. P., Platt, C. D., Chou, J., Benavides, F., Geha, R. S., & Segal, A. W. (2017). The LRRC8A mediated "swell activated" chloride conductance is dispensable for vacuolar homeostasis in neutrophils. *Frontiers in Pharmacology*, **8**, 262.

Ben Soussia, I., Mies, F., Naeije, R., & Shlyonsky, V. (2012). Melatonin down-regulates volume-sensitive chloride channels in fibroblasts. *Pflugers Archiv: European Journal of Physiology*, **464**(3), 273–285.

Bertelli, S., Remigante, A., Zuccolini, P., Barbieri, R., Ferrera, L., Picco, C., Gavazzo, P., & Pusch, M. (2021). Mechanisms of activation of LRRC8 volume regulated anion channels. *Cellular Physiology and Biochemistry*, **55**(S1), 41–56.

Bertelli, S., Zuccolini, P., Gavazzo, P., & Pusch, M. (2022). Molecular determinants underlying volume-regulated anion channel subunit-dependent oxidation sensitivity. *The Journal of Physiology*, **600**(17), 3965–3982.

Best, L., & Brown, P. D. (2009). Studies of the mechanism of activation of the volume-regulated anion channel in rat pancreatic $\beta$-cells. *Journal of Membrane Biology*, **230**(2), 83–91.

Bhat, E. A., & Sajjad, N. (2021). Human Pannexin 1 channel: Insight in structure–function mechanism and its potential physiological roles. *Molecular and Cellular Biochemistry*, **476**(3), 1529–1540.

Blest, H. T. W., Redmond, A., Avissar, J., Barker, J., Bridgeman, A., Fowler, G., Chauveau, L., Hertzog, J., Vendrell, I., Fischer, R., Iversen, M. B., Jing, L., Koelle, D. M., Paludan, S. R., Kessler, B. M., Crump, C. M., & Rehwinkel, J. (2024). HSV-1 employs UL56 to antagonize expression and function of cGAMP channels. *Cell Reports*, **43**(5), 114122.

Boese, S. H., Wehner, F., & Kinne, R. K. (1996). Taurine permeation through swelling-activated anion conductance in rat IMCD cells in primary culture. *American Journal of Physiology*, **271**(3 Pt 2), F498–507.

Bond, T., Basavappa, S., Christensen, M., & Strange, K. (1999). ATP dependence of the $I_{Cl,swell}$ channel varies with rate of cell swelling. Evidence for two modes of channel activation. *Journal of General Physiology*, **113**(3), 441–456.

Botchkin, L. M., & Matthews, G. (1993). Chloride current activated by swelling in retinal pigment epithelium cells. *American Journal of Physiology*, **265**(4 Pt 1), C1037–1045.

Bowens, N. H., Dohare, P., Kuo, Y. H., & Mongin, A. A. (2013). DCPIB, the proposed selective blocker of volume-regulated anion channels, inhibits several glutamate transport pathways in glial cells. *Molecular Pharmacology*, **83**(1), 22–32.

Bryan-Sisneros, A., Sabanov, V., Thoroed, S. M., & Doroshenko, P. (2000). Dual role of ATP in supporting volume-regulated chloride channels in mouse fibroblasts. *Biochimica et Biophysica Acta*, **1468**(1–2), 63–72.

Burendei, B., Shinozaki, R., Watanabe, M., Terada, T., Tani, K., Fujiyoshi, Y., & Oshima, A. (2020). Cryo-EM structures of undocked innexin-6 hemichannels in phospholipids. *Science Advances*, **6**(7), eaax3157.

Burow, P., Klapperstuck, M., & Markwardt, F. (2015). Activation of ATP secretion via volume-regulated anion channels by sphingosine-1-phosphate in RAW macrophages. *Pflugers Archiv: European Journal of Physiology*, **467**(6), 1215–1226.

Burow, P., & Markwardt, F. (2014). When S1P meets ATP. *Channels (Austin)*, **8**(5), 385–386.

Cahalan, M. D., & Chandy, K. G. (2009). The functional network of ion channels in T lymphocytes. *Immunological Reviews*, **231**(1), 59–87.

Cahalan, M. D., & Lewis, R. S. (1988). Role of potassium and chloride channels in volume regulation by T lymphocytes. *Society of General Physiologists Series*, **43**, 281–301.

Cannon, C. L., Basavappa, S., & Strange, K. (1998). Intracellular ionic strength regulates the volume sensitivity of a swelling-activated anion channel. *American Journal of Physiology*, **275**(2), C416–422.

Carozza, J. A., Bohnert, V., Nguyen, K. C., Skariah, G., Shaw, K. E., Brown, J. A., Rafat, M., von Eyben, R., Graves, E. E., Glenn, J. S., Smith, M., & Li, L. (2020). Extracellular cGAMP is a cancer cell-produced immunotransmitter involved in radiation-induced anti-cancer immunity. *Nature Cancer*, **1**(2), 184–196.

Carton, I., Trouet, D., Hermans, D., Barth, H., Aktories, K., Droogmans, G., Jorgensen, N. K., Hoffmann, E. K., Nilius, B., & Eggermont, J. (2002). RhoA exerts a permissive effect on volume-regulated anion channels in vascular endothelial cells. *American Journal of Physiology-Cell Physiology*, **283**(1), C115–125.

Cerboni, S., Jeremiah, N., Gentili, M., Gehrmann, U., Conrad, C., Stolzenberg, M. C., Picard, C., Neven, B., Fischer, A., Amigorena, S., Rieux-Laucat, F., & Manel, N. (2017). Intrinsic antiproliferative activity of the innate sensor STING in T lymphocytes. *Journal of Experimental Medicine*, **214**(6), 1769–1785.

Chen, J., Yang, J., Chu, J., Chen, K. H., Alt, J., Rais, R., & Qiu, Z. (2024). The SWELL1 channel promotes ischemic brain damage by mediating neuronal swelling and glutamate toxicity. *Advanced Science*, **11**(36), e2401085.

Chen, L., Konig, B., Liu, T., Pervaiz, S., Razzaque, Y. S., & Stauber, T. (2019). More than just a pressure relief valve: Physiological roles of volume-regulated LRRC8 anion channels. *Biological Chemistry*, **400**(11), 1481–1496.

Chen, X., Wang, L., Cao, L., Li, T., Li, Z., Sun, Y., Ding, J., Zhou, C., Xie, Y., Yue, N., Nan, J., Jia, X. M., Peng, C., Li, H., Yang, J., & Xiao, H. (2021). Regulation of anion channel LRRC8 volume-regulated anion channels in transport of 2'3'-cyclic GMP-AMP and cisplatin under steady state and inflammation. *Journal of Immunology*, **206**(9), 2061–2074.

Chirayath, T. W., Ollivier, M., Kayatekin, M., Rubera, I., Pham, C. N., Friard, J., Linck, N., Hirbec, H., Combes, C., Zarka, M., Liote, F., Richette, P., Rassendren, F., Compan, V., Duranton, C., & Ea, H. K. (2024). Activation of osmo-sensitive LRRC8 anion channels in macrophages is important for micro-crystallin joint inflammation. *Nature Communications*, **15**(1), 8179.

Choi, H., Miller, M. R., Nguyen, H. N., Rohrbough, J. C., Koch, S. R., Boatwright, N., Yarboro, M. T., Sah, R., McDonald, W. H., Reese, J. J., Stark, R. J., & Lamb, F. S. (2023). LRRC8A anion channels modulate vascular reactivity via association with myosin phosphatase rho interacting protein. *Federation of American Societies for Experimental Biology Journal*, **37**(7), e23028.

Chu, J., Yang, J., Zhou, Y., Chen, J., Chen, K. H., Zhang, C., Cheng, H. Y., Koylass, N., Liu, J. O., Guan, Y., & Qiu, Z. (2023). ATP-releasing SWELL1 channel in spinal microglia contributes to neuropathic pain. *Science Advances*, **9**(13), eade9931.

Compan, V., Baroja-Mazo, A., Lopez-Castejon, G., Gomez, A. I., Martinez, C. M., Angosto, D., Montero, M. T., Herranz, A. S., Bazan, E., Reimers, D., Mulero, V., & Pelegrin, P. (2012). Cell volume regulation modulates NLRP3 inflammasome activation. *Immunity*, **37**(3), 487–500.

Concepcion, A. R., Wagner, E., 2nd, Zhu, J., Tao, A. Y., Yang, J., Khodadadi-Jamayran, A., Wang, Y. H., Liu, M., Rose, R. E., Jones, D. R., Coetzee, W. A., Yule, D. I., & Feske, S. (2022). The volume-regulated anion channel LRRC8C suppresses T cell function by regulating cyclic dinucleotide transport and STING-p53 signaling. *Nature Immunology*, **23**(2), 287–302.

Cordova, A. F., Ritchie, C., Bohnert, V., & Li, L. (2021). Human SLC46A2 is the dominant cGAMP importer in extracellular cGAMP-sensing macrophages and monocytes. *American Chemical Society Central Science*, **7**(6), 1073–1088.

Corrales, L., Glickman, L. H., McWhirter, S. M., Kanne, D. B., Sivick, K. E., Katibah, G. E., Woo, S. R., Lemmens, E., Banda, T., Leong, J. J., Metchette, K., Dubensky, T. W. Jr., & Gajewski, T. F. (2015). Direct activation of STING in the tumor microenvironment leads to potent and systemic tumor regression and immunity. *Cell Reports*, **11**(7), 1018–1030.

Crepel, V., Panenka, W., Kelly, M. E., & MacVicar, B. A. (1998). Mitogen-activated protein and tyrosine kinases in the activation of astrocyte volume-activated chloride current. *Journal of Neuroscience*, **18**(4), 1196–1206.

Danilchanka, O., & Mekalanos, J. J. (2013). Cyclic dinucleotides and the innate immune response. *Cell*, **154**(5), 962–970.

Decher, N., Lang, H. J., Nilius, B., Bruggemann, A., Busch, A. E., & Steinmeyer, K. (2001). DCPIB is a novel selective blocker of $I_{Cl,swell}$ and prevents swelling-induced shortening of guinea-pig atrial action potential duration. *British Journal of Pharmacology*, **134**(7), 1467–1479.

Deneka, D., Rutz, S., Hutter, C. A. J., Seeger, M. A., Sawicka, M., & Dutzler, R. (2021). Allosteric modulation of LRRC8 channels by targeting their cytoplasmic domains. *Nature Communications*, **12**(1), 5435.

Deneka, D., Sawicka, M., Lam, A. K. M., Paulino, C., & Dutzler, R. (2018). Structure of a volume-regulated anion channel of the LRRC8 family. *Nature*, **558**(7709), 254–259.

Deng, L., Liang, H., Xu, M., Yang, X., Burnette, B., Arina, A., Li, X. D., Mauceri, H., Beckett, M., Darga, T., Huang, X., Gajewski, T. F., Chen, Z. J., Fu, Y. X., & Weichselbaum, R. R. (2014). STING-dependent cytosolic DNA sensing promotes radiation-induced type I interferon-dependent antitumor immunity in immunogenic tumors. *Immunity*, **41**(5), 843–852.

Deng, W., Mahajan, R., Baumgarten, C. M., & Logothetis, D. E. (2016). The $I_{Cl,swell}$ inhibitor DCPIB blocks Kir channels that possess weak affinity for $PIP_2$. *Pflugers Archiv: European journal of Physiology*, **468**(5), 817–824.

Deng, Z., He, Z., Maksaev, G., Bitter, R. M., Rau, M., Fitzpatrick, J. A. J., & Yuan, P. (2020). Cryo-EM structures of the ATP release channel pannexin 1. *Nature Structural & Molecular Biology*, **27**(4), 373–381.

Droogmans, G., Maertens, C., Prenen, J., & Nilius, B. (1999). Sulphonic acid derivatives as probes of pore properties of volume-regulated anion channels in endothelial cells. *British Journal of Pharmacology*, **128**(1), 35–40.

Du, X. L., Gao, Z., Lau, C. P., Chiu, S. W., Tse, H. F., Baumgarten, C. M., & Li, G. R. (2004). Differential effects of tyrosine kinase inhibitors on volume-sensitive chloride current in human atrial myocytes: Evidence for dual regulation by Src and EGFR kinases. *Journal of General Physiology*, **123**(4), 427–439.

Emma, F., McManus, M., & Strange, K. (1997). Intracellular electrolytes regulate the volume set point of the organic osmolyte/anion channel VSOAC. *American Journal of Physiology*, **272**(6 Pt 1), C1766–1775.

Estevez, A. Y., Bond, T., & Strange, K. (2001). Regulation of $I_{Cl,swell}$ in neuroblastoma cells by G protein signaling pathways. *American Journal of Physiology-Cell Physiology*, **281**(1), C89–98.

Feske, S., Concepcion, A. R., & Coetzee, W. A. (2019). Eye on ion channels in immune cells. *Science Signaling*, **12**(572).

Feske, S., Wulff, H., & Skolnik, E. Y. (2015). Ion channels in innate and adaptive immunity. *Annual Review of Immunology*, **33**, 291–353.

Fujii, T., Takahashi, Y., Takeshima, H., Saitoh, C., Shimizu, T., Takeguchi, N., & Sakai, H. (2015). Inhibition of gastric $H^+$,$K^+$-ATPase by 4-(2-butyl-6, 7-dichloro-2-cyclopentylindan-1-on-5-yl)oxybutyric acid (DCPIB), an inhibitor of volume-regulated anion channel. *European Journal of Pharmacology*, **765**, 34–41.

Furman, D., Campisi, J., Verdin, E., Carrera-Bastos, P., Targ, S., Franceschi, C., Ferrucci, L., Gilroy, D. W., Fasano, A., Miller, G. W., Miller, A. H., Mantovani, A., Weyand, C. M., Barzilai, N., Goronzy, J. J., Rando, T. A., Effros, R. B., Lucia, A., Kleinstreuer, N., & Slavich, G. M. (2019). Chronic inflammation in the etiology of disease across the life span. *Nature Medicine*, **25**(12), 1822–1832.

Gaete, P. S., Kumar, D., Fernandez, C. I., Valdez Capuccino, J. M., Bhatt, A., Jiang, W., Lin, Y. C., Liu, Y., Harris, A. L., Luo, Y. L., & Contreras, J. E. (2024). Large-pore connexin hemichannels function like molecule transporters independent of ion conduction. *Proceedings of the National Academy of Sciences, USA*, **121**(33), e2403903121.

Gaitan-Penas, H., Gradogna, A., Laparra-Cuervo, L., Solsona, C., Fernandez-Duenas, V., Barrallo-Gimeno, A., Ciruela, F., Lakadamyali, M., Pusch, M., & Estevez, R. (2016). Investigation of LRRC8-mediated volume-regulated anion currents in *Xenopus Oocytes*. *Biophysical Journal*, **111**(7), 1429–1443.

Gajewski, T. F., & Higgs, E. F. (2020). Immunotherapy with a sting. *Science*, **369**(6506), 921–922.

Geltink, R. I. K., Kyle, R. L., & Pearce, E. L. (2018). Unraveling the complex interplay between T cell metabolism and function. *Annual Review of Immunology*, **36**, 461–488.

Gogoi, H., Mansouri, S., & Jin, L. (2020). The age of cyclic dinucleotide vaccine adjuvants. *Vaccines (Basel)*, **8**(1), 453.

Gradogna, A., Gavazzo, P., Boccaccio, A., & Pusch, M. (2017). Subunit-dependent oxidative stress sensitivity of LRRC8 volume-regulated anion channels. *The Journal of Physiology*, **595**(21), 6719–6733.

Green, J. P., Swanton, T., Morris, L. V., El-Sharkawy, L. Y., Cook, J., Yu, S., Beswick, J., Adamson, A. D., Humphreys, N. E., Bryce, R., Freeman, S., Lawrence, C., & Brough, D. (2020). LRRC8A is essential for hypotonicity-, but not for DAMP-induced NLRP3 inflammasome activation. *eLife*, **9**, e59704.

Grinstein, S., Clarke, C. A., Dupre, A., & Rothstein, A. (1982). Volume-induced increase of anion permeability in human lymphocytes. *Journal of General Physiology*, **80**(6), 801–823.

Grinstein, S., Clarke, C. A., & Rothstein, A. (1982). Increased anion permeability during volume regulation in human lymphocytes. *Philosophical Transactions of the Royal Society of London-Series B: Biological Sciences*, **299**(1097), 509–518.

Grinstein, S., Clarke, C. A., Rothstein, A., & Gelfand, E. W. (1983). Volume-induced anion conductance in human B lymphocytes is cation independent. *American Journal of Physiology*, **245**(1), C160–163.

Gulen, M. F., Koch, U., Haag, S. M., Schuler, F., Apetoh, L., Villunger, A., Radtke, F., & Ablasser, A. (2017). Signalling strength determines proapoptotic functions of STING. *Nature Communications*, **8**, 427.

Gunasekar, S. K., Xie, L., Kumar, A., Hong, J., Chheda, P. R., Kang, C., Kern, D. M., My-Ta, C., Maurer, J., Heebink, J., Gerber, E. E., Grzesik, W. J., Elliot-Hudson, M., Zhang, Y., Key, P., Kulkarni, C. A., Beals, J. W., Smith, G. I., Samuel, I., Smith, J. K., Nau, P., Imai, Y., Sheldon, R. D., Taylor, E. B., Lerner, D. J., Norris, A. W., Klein, S., Brohawn, S. G., Kerns, R., & Sah, R. (2022). Small molecule SWELL1 complex induction improves glycemic control and non-alcoholic fatty liver disease in murine Type 2 diabetes. *Nature Communications*, **13**(1), 784.

Hayashi, T., Nozaki, Y., Nishizuka, M., Ikawa, M., Osada, S., & Imagawa, M. (2011). Factor for adipocyte differentiation 158 gene disruption prevents the body weight gain and insulin resistance induced by a high-fat diet. *Biological & Pharmaceutical Bulletin*, **34**(8), 1257–1263.

Hazama, A., & Okada, Y. (1988). $Ca^{2+}$ sensitivity of volume-regulatory $K^+$ and $Cl^-$ channels in cultured human epithelial cells. *The Journal of Physiology*, **402**, 687–702.

He, W., Henne, A., Lauterbach, M., Geissmar, E., Nikolka, F., Kho, C., Heinz, A., Dostert, C., Grusdat, M., Cordes, T., Harm, J., Goldmann, O., Ewen, A., Verschueren, C., Blay-Cadanet, J., Geffers, R., Garritsen, H., Kneiling, M., Holm, C. K., Metallo, C. M., Medina, E., Abdullah, Z., Latz, E., Brenner, D., & Hiller, K. (2022). Mesaconate is synthesized from itaconate and exerts immunomodulatory effects in macrophages. *Nature Metabolism*, **4**(5), 524–533.

Hermoso, M., Olivero, P., Torres, R., Riveros, A., Quest, A. F., & Stutzin, A. (2004). Cell volume regulation in response to hypotonicity is impaired in HeLa cells expressing a protein kinase C $\alpha$ mutant lacking kinase activity. *Journal of Biological Chemistry*, **279**(17), 17681–17689.

Hoffmann, E. K. (1978). Regulation of cell volume by selective changes in the leak permeabilities of Ehrlich ascites tumor cells. *In*: *Alfred Benzon Symposium XI Osmotic and Volume Regulation CB Jørgensen and E Skadhauge, eds*, 397–417.

Hoffmann, E. K., Lambert, I. H., & Pedersen, S. F. (2009). Physiology of cell volume regulation in vertebrates. *Physiological Reviews*, **89**(1), 193–277.

Hooftman, A., Angiari, S., Hester, S., Corcoran, S. E., Runtsch, M. C., Ling, C., Ruzek, M. C., Slivka, P. F., McGettrick, A. F., Banahan, K., Hughes, M. M., Irvine, A. D., Fischer, R., & O'Neill, L. A. J. (2020). The immunomodulatory metabolite itaconate modifies NLRP3 and inhibits inflammasome activation. *Cell Metabolism*, **32**(3), 468–478 e467.

Hyzinski-Garcia, M. C., Rudkouskaya, A., & Mongin, A. A. (2014). LRRC8A protein is indispensable for swelling-activated and ATP-induced release of excitatory amino acids in rat astrocytes. *The Journal of Physiology*, **592**(22), 4855–4862.

Imanishi, T., Unno, M., Kobayashi, W., Yoneda, N., Matsuda, S., Ikeda, K., Hoshii, T., Hirao, A., Miyake, K., Barber, G. N., Arita, M., Ishii, K. J., Akira, S., & Saito, T. (2019). Reciprocal regulation of STING and TCR signaling by mTORC1 for T-cell activation and function. *Life Science Alliance*, **2**(1), e201800282.

Jackson, P. S., Churchwell, K., Ballatori, N., Boyer, J. L., & Strange, K. (1996). Swelling-activated anion conductance in skate hepatocytes: Regulation by cell $Cl^-$ and ATP. *American Journal of Physiology*, **270**(1 Pt 1), C57–66.

Jackson, P. S., Morrison, R., & Strange, K. (1994). The volume-sensitive organic osmolyte-anion channel VSOAC is regulated by nonhydrolytic ATP binding. *American Journal of Physiology*, **267**(5 Pt 1), C1203–1209.

Jackson, P. S., & Strange, K. (1993). Volume-sensitive anion channels mediate swelling-activated inositol and taurine efflux. *American Journal of Physiology*, **265**(6 Pt 1), C1489–1500.

Jackson, P. S., & Strange, K. (1996). Single channel properties of a volume sensitive anion channel: Lessons from noise analysis. *Kidney International*, **49**(6), 1695–1699.

Jentsch, T. J. (2016). VRACs and other ion channels and transporters in the regulation of cell volume and beyond. *Nature Reviews Molecular Cell Biology*, **17**(5), 293–307.

Jin, Q., Zhang, B., Zheng, X., Li, N., Xu, L., Xie, Y., Song, F., Bhat, E. A., Chen, Y., Gao, N., Guo, J., Zhang, X., & Ye, S. (2020). Cryo-EM structures of human pannexin 1 channel. *Cell Research*, **30**(5), 449–451.

Ju, L., Chen, Y., Xue, L., Du, X., & Zhu, C. (2016). Cooperative unfolding of distinctive mechanoreceptor domains transduces force into signals. *eLife*, **5**, e15447.

Ju, L., Lou, J., Chen, Y., Li, Z., & Zhu, C. (2015). Force-induced unfolding of leucine-rich repeats of glycoprotein Ib$\alpha$ strengthens ligand interaction. *Biophysical Journal*, **109**(9), 1781–1784.

Kasuya, G., Nakane, T., Yokoyama, T., Jia, Y., Inoue, M., Watanabe, K., Nakamura, R., Nishizawa, T., Kusakizako, T., Tsutsumi, A., Yanagisawa, H., Dohmae, N., Hattori, M., Ichijo, H., Yan, Z., Kikkawa, M., Shirouzu, M., Ishitani, R., & Nureki, O. (2018). Cryo-EM structures of the human volume-regulated anion channel LRRC8. *Nature Structural & Molecular Biology*, **25**(9), 797–804.

Kay, A. R., & Blaustein, M. P. (2019). Evolution of our understanding of cell volume regulation by the pump-leak mechanism. *Journal of General Physiology*, **151**(4), 407–416.

Kefauver, J. M., Saotome, K., Dubin, A. E., Pallesen, J., Cottrell, C. A., Cahalan, S. M., Qiu, Z., Hong, G., Crowley, C. S., Whitwam, T., Lee, W. H., Ward, A. B., & Patapoutian, A. (2018). Structure of the human volume regulated anion channel. *eLife*, **7**, e38461.

Kern, D. M., Bleier, J., Mukherjee, S., Hill, J. M., Kossiakoff, A. A., Isacoff, E. Y., & Brohawn, S. G. (2023). Structural basis for assembly and lipid-mediated gating of LRRC8A:C volume-regulated anion channels. *Nature Structural & Molecular Biology*, **30**(6), 841–852.

Kern, D. M., Oh, S., Hite, R. K., & Brohawn, S. G. (2019). Cryo-EM structures of the DCPIB-inhibited volume-regulated anion channel LRRC8A in lipid nanodiscs. *eLife*, **8**, e42636.

Kobe, B., & Kajava, A. V. (2001). The leucine-rich repeat as a protein recognition motif. *Current Opinion in Structural Biology*, **11**(6), 725–732.

Konig, B., Hao, Y., Schwartz, S., Plested, A. J., & Stauber, T. (2019). A FRET sensor of C-terminal movement reveals VRAC activation by plasma membrane DAG signaling rather than ionic strength. *eLife*, **8**, e45421.

Kostritskaia, Y., Pervaiz, S., Klemmer, A., Klussendorf, M., & Stauber, T. (2024). Sphingosine-1-phosphate activates LRRC8 volume-regulated anion channels through G$\beta\gamma$ signalling. *The Journal of Physiology*. Advance online publication. https://doi.org/10.1113/JP286665.

Kubota, K., Kim, J. Y., Sawada, A., Tokimasa, S., Fujisaki, H., Matsuda-Hashii, Y., Ozono, K., & Hara, J. (2004). LRRC8 involved in B cell development belongs to a novel family of leucine-rich repeat proteins. *Febs Letters*, **564**(1–2), 147–152.

Kuhl, N., Linder, A., Philipp, N., Nixdorf, D., Fischer, H., Veth, S., Kuut, G., Xu, T. T., Theurich, S., Carell, T., Subklewe, M., & Hornung, V. (2023). STING agonism turns human T cells into interferon-producing cells but impedes their functionality. *EMBO Reports*, **24**(3), e55536.

Kumar, A., Xie, L., Ta, C. M., Hinton, A. O., Gunasekar, S. K., Minerath, R. A., Shen, K., Maurer, J. M., Grueter, C. E., Abel, E. D., Meyer, G., & Sah, R. (2020). SWELL1 regulates skeletal muscle cell size, intracellular signaling, adiposity and glucose metabolism. *eLife*, **9**, e58941.

Kumar, L., Chou, J., Yee, C. S., Borzutzky, A., Vollmann, E. H., von Andrian, U. H., Park, S. Y., Hollander, G., Manis, J. P., Poliani, P. L., & Geha, R. S. (2014). Leucine-rich repeat containing 8A (LRRC8A) is essential for T lymphocyte development and function. *Journal of Experimental Medicine*, **211**(5), 929–942.

Kuzuya, M., Hirano, H., Hayashida, K., Watanabe, M., Kobayashi, K., Terada, T., Mahmood, M. I., Tama, F., Tani, K., Fujiyoshi, Y., & Oshima, A. (2022). Structures of human pannexin-1 in nanodiscs reveal gating mediated by dynamic movement of the N terminus and phospholipids. *Science Signaling*, **15**(720), eabg6941.

Lahey, L. J., Mardjuki, R. E., Wen, X., Hess, G. T., Ritchie, C., Carozza, J. A., Bohnert, V., Maduke, M., Bassik, M. C., & Li, L. (2020). LRRC8A:C/E heteromeric channels are ubiquitous transporters of cGAMP. *Molecular Cell*, **80**(4), 578–591 e575.

Lalouette, A., Lablack, A., Guenet, J. L., Montagutelli, X., & Segretain, D. (1996). Male sterility caused by sperm cell-specific structural abnormalities in *ebouriffe*, a new mutation of the house mouse. *Biology of Reproduction*, **55**(2), 355–363.

Lanng, K. R. B., Lauridsen, E. L., & Jakobsen, M. R. (2024). The balance of STING signaling orchestrates immunity in cancer. *Nature Immunology*, **25**(7), 1144–1157.

Larkin, B., Ilyukha, V., Sorokin, M., Buzdin, A., Vannier, E., & Poltorak, A. (2017). Cutting edge: Activation of STING in T cells induces type I IFN responses and cell death. *Journal of Immunology*, **199**(2), 397–402.

Lee, C. C., Freinkman, E., Sabatini, D. M., & Ploegh, H. L. (2014). The protein synthesis inhibitor blasticidin s enters mammalian cells via leucine-rich repeat-containing protein 8D. *Journal of Biological Chemistry*, **289**(24), 17124–17131.

Lepple-Wienhues, A., Szabo, I., Laun, T., Kaba, N. K., Gulbins, E., & Lang, F. (1998). The tyrosine kinase p56$^{lck}$ mediates activation of swelling-induced chloride channels in lymphocytes. *Journal of Cell Biology*, **141**(1), 281–286.

Lewis, R. S., Ross, P. E., & Cahalan, M. D. (1993). Chloride channels activated by osmotic stress in T lymphocytes. *Journal of General Physiology*, **101**(6), 801–826.

Li, D., & Wu, M. (2021). Pattern recognition receptors in health and diseases. *Signal Transduction and Targeted Therapy*, **6**(1), 291.

Li, Z., Zheng, W., Kong, W., & Zeng, T. (2023). Itaconate: A potent macrophage immunomodulator. *Inflammation*, **46**(4), 1177–1191.

Liu, H., Polovitskaya, M. M., Yang, L., Li, M., Li, H., Han, Z., Wu, J., Zhang, Q., Jentsch, T. J., & Liao, J. (2023). Structural insights into anion selectivity and activation mechanism of LRRC8 volume-regulated anion channels. *Cell Reports*, **42**(8), 112926.

Lopez-Cayuqueo, K. I., Planells-Cases, R., Pietzke, M., Oliveras, A., Kempa, S., Bachmann, S., & Jentsch, T. J. (2022). Renal deletion of LRRC8/VRAC channels induces proximal tubulopathy. *Journal of the American Society of Nephrology*, **33**(8), 1528–1545.

Luteijn, R. D., Zaver, S. A., Gowen, B. G., Wyman, S. K., Garelis, N. E., Onia, L., McWhirter, S. M., Katibah, G. E., Corn, J. E., Woodward, J. J., & Raulet, D. H. (2019). SLC19A1 transports immunoreactive cyclic dinucleotides. *Nature*, **573**(7774), 434–438.

Lutter, D., Ullrich, F., Lueck, J. C., Kempa, S., & Jentsch, T. J. (2017). Selective transport of neurotransmitters and modulators by distinct volume-regulated LRRC8 anion channels. *Journal of Cell Science*, **130**(6), 1122–1133.

Lv, J., Liang, Y., Zhang, S., Lan, Q., Xu, Z., Wu, X., Kang, L., Ren, J., Cao, Y., Wu, T., Lin, K. L., Yung, K. K. L., Cao, X., Pang, J., & Zhou, P. (2019). DCPIB, an inhibitor of volume-regulated anion channels, distinctly modulates $K_2P$ channels. *Acs Chemical Neuroscience*, **10**(6), 2786–2793.

Maltbaek, J. H., Cambier, S., Snyder, J. M., & Stetson, D. B. (2022). ABCC1 transporter exports the immuno-stimulatory cyclic dinucleotide cGAMP. *Immunity*, **55**(10), 1799–1812.e4.

Manolopoulos, V. G., Voets, T., Declercq, P. E., Droogmans, G., & Nilius, B. (1997). Swelling-activated efflux of taurine and other organic osmolytes in endothelial cells. *American Journal of Physiology*, **273**(1 Pt 1), C214–222.

Marcus, A., Mao, A. J., Lensink-Vasan, M., Wang, L., Vance, R. E., & Raulet, D. H. (2018). Tumor-derived cGAMP triggers a STING-mediated interferon response in non-tumor cells to activate the NK cell response. *Immunity*, **49**(4), 754–763 e754.

Marcus, Y. (1988). Ionic radii in aqueous solutions. *Chemical Reviews*, **88**(8), 1475–1498.

Margolis, S. R., Wilson, S. C., & Vance, R. E. (2017). Evolutionary origins of cGAS-STING signaling. *Trends in Immunology*, **38**(10), 733–743.

McFadden, B. A., & Purohit, S. (1977). Itaconate, an isocitrate lyase-directed inhibitor in *Pseudomonas indigofera*. *Journal of Bacteriology*, **131**(1), 136–144.

Michalski, K., Syrjanen, J. L., Henze, E., Kumpf, J., Furukawa, H., & Kawate, T. (2020). The Cryo-EM structure of pannexin 1 reveals unique motifs for ion selection and inhibition. *eLife*, **9**, e54670.

Moremen, K. W., Tiemeyer, M., & Nairn, A. V. (2012). Vertebrate protein glycosylation: Diversity, synthesis and function. *Nature Reviews Molecular Cell Biology*, **13**(7), 448–462.

Mou, L., Ke, M., Song, M., Shan, Y., Xiao, Q., Liu, Q., Li, J., Sun, K., Pu, L., Guo, L., Geng, J., Wu, J., & Deng, D. (2020). Structural basis for gating mechanism of Pannexin 1 channel. *Cell Research*, **30**(5), 452–454.

Nakamura, R., Numata, T., Kasuya, G., Yokoyama, T., Nishizawa, T., Kusakizako, T., Kato, T., Hagino, T., Dohmae, N., Inoue, M., Watanabe, K., Ichijo, H., Kikkawa, M., Shirouzu, M., Jentsch, T. J., Ishitani, R., Okada, Y., & Nureki, O. (2020). Cryo-EM structure of the volume-regulated anion channel LRRC8D isoform identifies features important for substrate permeation. *Communications Biology*, **3**(1), 240.

Nilius, B., Eggermont, J., Voets, T., Buyse, G., Manolopoulos, V., & Droogmans, G. (1997). Properties of volume-regulated anion channels in mammalian cells. *Progress in Biophysics and Molecular Biology*, **68**(1), 69–119.

Nilius, B., Oike, M., Zahradnik, I., & Droogmans, G. (1994). Activation of a $Cl^-$ current by hypotonic volume increase in human endothelial cells. *Journal of General Physiology*, **103**(5), 787–805.

Nilius, B., Prenen, J., Voets, T., Eggermont, J., & Droogmans, G. (1998). Activation of volume-regulated chloride currents by reduction of intracellular ionic strength in bovine endothelial cells. *The Journal of Physiology*, **506**(Pt 2), 353–361.

Nilius, B., Sehrer, J., & Droogmans, G. (1994). Permeation properties and modulation of volume-activated $Cl^-$ currents in human endothelial cells. *British Journal of Pharmacology*, **112**(4), 1049–1056.

Okada, Y. (2024a). Physiology of the volume-sensitive/regulatory anion channel VSOR/VRAC: Part 2: Its activation mechanisms and essential roles in organic signal release. *Journal of Physiological Sciences*, **74**(1), 34.

Okada, Y. (2024b). Physiology of the volume-sensitive/regulatory anion channel VSOR/VRAC. Part 1: From its discovery and phenotype characterization to the molecular entity identification. *Journal of Physiological Sciences*, **74**(1), 3.

Olona, A., Leishman, S., & Anand, P. K. (2022). The NLRP3 inflammasome: Regulation by metabolic signals. *Trends in Immunology*, **43**(12), 978–989.

Osei-Owusu, J., Yang, J., Vitery, M. D. C., & Qiu, Z. (2018). Molecular biology and physiology of volume-regulated anion channel (VRAC). *Current Topics in Membranes*, **81**, 177–203.

Perregaux, D. G., Laliberte, R. E., & Gabel, C. A. (1996). Human monocyte interleukin-1$\beta$ posttranslational processing. Evidence of a volume-regulated response. *Journal of Biological Chemistry*, **271**(47), 29830–29838.

Pervaiz, S., Kopp, A., von Kleist, L., & Stauber, T. (2019). Absolute protein amounts and relative abundance of volume-regulated anion channel (VRAC) LRRC8 subunits in cells and tissues revealed by quantitative immunoblotting. *International Journal of Molecular Sciences*, **20**(23), 5879.

Planells-Cases, R., Lutter, D., Guyader, C., Gerhards, N. M., Ullrich, F., Elger, D. A., Kucukosmanoglu, A., Xu, G., Voss, F. K., Reincke, S. M., Stauber, T., Blomen, V. A., Vis, D. J., Wessels, L. F., Brummelkamp, T. R., Borst, P., Rottenberg, S., & Jentsch, T. J. (2015). Subunit composition of VRAC channels determines substrate specificity and cellular resistance to Pt-based anti-cancer drugs. *European Molecular Biology Organization Journal*, **34**(24), 2993–3008.

Platt, C. D., Chou, J., Houlihan, P., Badran, Y. R., Kumar, L., Bainter, W., Poliani, P. L., Perez, C. J., Dent, S. Y. R., Clapham, D. E., Benavides, F., & Geha, R. S. (2017). Leucine-rich repeat containing 8A (LRRC8A)-dependent volume-regulated anion channel activity is dispensable for T-cell development and function. *Journal of Allergy and Clinical Immunology*, **140**(6), 1651–1659 e1651.

Platt, R. J., Chen, S., Zhou, Y., Yim, M. J., Swiech, L., Kempton, H. R., Dahlman, J. E., Parnas, O., Eisenhaure, T. M., Jovanovic, M., Graham, D. B., Jhunjhunwala, S., Heidenreich, M., Xavier, R. J., Langer, R., Anderson, D. G., Hacohen, N., Regev, A., Feng, G., Sharp, P. A., & Zhang, F. (2014). CRISPR-Cas9 knockin mice for genome editing and cancer modeling. *Cell*, **159**(2), 440–455.

Poletto Chaves, L. A., & Varanda, W. A. (2008). Volume-activated chloride channels in mice Leydig cells. *Pflugers Archiv: European Journal of Physiology*, **457**(2), 493–504.

Qin, W., Qin, K., Zhang, Y., Jia, W., Chen, Y., Cheng, B., Peng, L., Chen, N., Liu, Y., Zhou, W., Wang, Y. L., Chen, X., & Wang, C. (2019). S-glycosylation-based cysteine profiling reveals regulation of glycolysis by itaconate. *Nature Chemical Biology*, **15**(10), 983–991.

Qiu, Z., Dubin, A. E., Mathur, J., Tu, B., Reddy, K., Miraglia, L. J., Reinhardt, J., Orth, A. P., & Patapoutian, A. (2014). SWELL1, a plasma membrane protein, is an essential component of volume-regulated anion channel. *Cell*, **157**(2), 447–458.

Qu, R., Dong, L., Zhang, J., Yu, X., Wang, L., & Zhu, S. (2020). Cryo-EM structure of human heptameric Pannexin 1 channel. *Cell Research*, **30**(5), 446–448.

Ren, Z., & Baumgarten, C. M. (2005). Antagonistic regulation of swelling-activated $Cl^-$ current in rabbit ventricle by Src and EGFR protein tyrosine kinases. *American Journal of Physiology-Heart and Circulatory Physiology*, **288**(6), H2628–2636.

Ritchie, C., Cordova, A. F., Hess, G. T., Bassik, M. C., & Li, L. (2019). SLC19A1 is an importer of the immunotransmitter cGAMP. *Molecular Cell*, **75**(2), 372–381 e375.

Rittenhouse, J. W., & McFadden, B. A. (1974). Inhibition of isocitrate lyase from *Pseudomonas indigofera* by itaconate. *Archives of Biochemistry and Biophysics*, **163**(1), 79–86.

Roman, R. M., Bodily, K. O., Wang, Y., Raymond, J. R., & Fitz, J. G. (1998). Activation of protein kinase C $\alpha$ couples cell volume to membrane $Cl^-$ permeability in HTC hepatoma and Mz-ChA-1 cholangiocarcinoma cells. *Hepatology*, **28**(4), 1073–1080.

Ruan, Z., Orozco, I. J., Du, J., & Lu, W. (2020). Structures of human pannexin 1 reveal ion pathways and mechanism of gating. *Nature*, **584**(7822), 646–651.

Rudkouskaya, A., Chernoguz, A., Haskew-Layton, R. E., & Mongin, A. A. (2008). Two conventional protein kinase C isoforms, $\alpha$ and $\beta$ I, are involved in the ATP-induced activation of volume-regulated anion channel and glutamate release in cultured astrocytes. *Journal of Neurochemistry*, **105**(6), 2260–2270.

Rutz, S., Deneka, D., Dittmann, A., Sawicka, M., & Dutzler, R. (2023). Structure of a volume-regulated heteromeric LRRC8A/C channel. *Nature Structural & Molecular Biology*, **30**(1), 52–61.

Sabirov, R. Z., Prenen, J., Tomita, T., Droogmans, G., & Nilius, B. (2000). Reduction of ionic strength activates single volume-regulated anion channels (VRAC) in endothelial cells. *Pflugers Archiv: European Journal of Physiology*, **439**(3), 315–320.

Samson, N., & Ablasser, A. (2022). The cGAS-STING pathway and cancer. *Nature Cancer*, **3**(12), 1452–1463.

Sawada, A., Takihara, Y., Kim, J. Y., Matsuda-Hashii, Y., Tokimasa, S., Fujisaki, H., Kubota, K., Endo, H., Onodera, T., Ohta, H., Ozono, K., & Hara, J. (2003). A congenital mutation of the novel gene LRRC8 causes agammaglobulinemia in humans. *Journal of Clinical Investigation*, **112**(11), 1707–1713.

Schober, A. L., Wilson, C. S., & Mongin, A. A. (2017). Molecular composition and heterogeneity of the LRRC8-containing swelling-activated osmolyte channels in primary rat astrocytes. *The Journal of Physiology*, **595**(22), 6939–6951.

Shimizu, T., Numata, T., & Okada, Y. (2004). A role of reactive oxygen species in apoptotic activation of volume-sensitive $Cl^-$ channel. *Proceedings of the National Academy of Sciences, USA*, **101**(17), 6770–6773.

Shlyonsky, V., Soussia, I. B., Naeije, R., & Mies, F. (2011). Opposing effects of bone morphogenetic protein-2 and endothelin-1 on lung fibroblast chloride currents. *American Journal of Respiratory Cell and Molecular Biology*, **45**(6), 1154–1160.

Sorota, S. (1995). Tyrosine protein kinase inhibitors prevent activation of cardiac swelling-induced chloride current. *Pflugers Archiv: European Journal of Physiology*, **431**(2), 178–185.

Stein, W. D. (1995). The sodium pump in the evolution of animal cells. *Philosophical Transactions of the Royal Society of London-Series B: Biological Sciences*, **349**(1329), 263–269.

Strange, K., Yamada, T., & Denton, J. S. (2019). A 30-year journey from volume-regulated anion currents to molecular structure of the LRRC8 channel. *Journal of General Physiology*, **151**(2), 100–117.

Strelko, C. L., Lu, W., Dufort, F. J., Seyfried, T. N., Chiles, T. C., Rabinowitz, J. D., & Roberts, M. F. (2011). Itaconic acid is a mammalian metabolite induced during macrophage activation. *Journal of the American Chemical Society*, **133**(41), 16386–16389.

Sugimoto, M. S.H., Yokote, Y., Onuma, H., Kaneko, M., Mori, M., Sakaguchi, Y., Soga, T., & Tomita, M. (2012). Non-targeted metabolite profiling in activated macrophage secretion. *Metabolomics*, **8**, 624–633.

Sun, L., Wu, J., Du, F., Chen, X., & Chen, Z. J. (2013). Cyclic GMP-AMP synthase is a cytosolic DNA sensor that activates the type I interferon pathway. *Science*, **339**(6121), 786–791.

Swain, A., Bambouskova, M., Kim, H., Andhey, P. S., Duncan, D., Auclair, K., Chubukov, V., Simons, D. M., Roddy, T. P., Stewart, K. M., & Artyomov, M. N. (2020). Comparative evaluation of itaconate and its derivatives reveals divergent inflammasome and type I interferon regulation in macrophages. *Nature Metabolism*, **2**(7), 594–602.

Syeda, R., Qiu, Z., Dubin, A. E., Murthy, S. E., Florendo, M. N., Mason, D. E., Mathur, J., Cahalan, S. M., Peters, E. C., Montal, M., & Patapoutian, A. (2016). LRRC8 proteins form volume-regulated anion channels that sense ionic strength. *Cell*, **164**(3), 499–511.

Takahashi, H., Yamada, T., Denton, J. S., Strange, K., & Karakas, E. (2023). Cryo-EM structures of an LRRC8 chimera with native functional properties reveal heptameric assembly. *eLife*, **12**, e82431.

Ternovsky, V. I., Okada, Y., & Sabirov, R. Z. (2004). Sizing the pore of the volume-sensitive anion channel by differential polymer partitioning. *Febs Letters*, **576**(3), 433–436.

Thoroed, S. M., Bryan-Sisneros, A., & Doroshenko, P. (1999). Protein phosphotyrosine phosphatase inhibitors suppress regulatory volume decrease and the volume-sensitive $Cl^-$ conductance in mouse fibroblasts. *Pflugers Archiv: European Journal of Physiology*, **438**(2), 133–140.

Tilly, B. C., Edixhoven, M. J., Tertoolen, L. G., Morii, N., Saitoh, Y., Narumiya, S., & de Jonge, H. R. (1996). Activation of the osmo-sensitive chloride conductance involves $p21^{rho}$ and is accompanied by a transient reorganization of the F-actin cytoskeleton. *Molecular Biology of the Cell*, **7**(9), 1419–1427.

Tilly, B. C., van den Berghe, N., Tertoolen, L. G., Edixhoven, M. J., & de Jonge, H. R. (1993). Protein tyrosine phosphorylation is involved in osmoregulation of ionic conductances. *Journal of Biological Chemistry*, **268**(27), 19919–19922.

Ullrich, F., Reincke, S. M., Voss, F. K., Stauber, T., & Jentsch, T. J. (2016). Inactivation and anion selectivity of volume-regulated anion channels (VRACs) depend on C-terminal residues of the first extracellular loop. *Journal of Biological Chemistry*, **291**(33), 17040–17048.

Varela, D., Simon, F., Riveros, A., Jorgensen, F., & Stutzin, A. (2004). NAD(P)H oxidase-derived $H_2O_2$ signals chloride channel activation in cell volume regulation and cell proliferation. *Journal of Biological Chemistry*, **279**(14), 13301–13304.

Voets, T., Droogmans, G., Raskin, G., Eggermont, J., & Nilius, B. (1999). Reduced intracellular ionic strength as the initial trigger for activation of endothelial volume-regulated anion channels. *Proceedings of the National Academy of Sciences, USA*, **96**(9), 5298–5303.

Voets, T., Manolopoulos, V., Eggermont, J., Ellory, C., Droogmans, G., & Nilius, B. (1998). Regulation of a swelling-activated chloride current in bovine endothelium by protein tyrosine phosphorylation and G proteins. *The Journal of Physiology*, **506**(Pt 2), 341–352.

von Weikersthal, S. F., Barrand, M. A., & Hladky, S. B. (1999). Functional and molecular characterization of a volume-sensitive chloride current in rat brain endothelial cells. *The Journal of Physiology*, **516**(Pt 1), 75–84.

Voss, F. K., Ullrich, F., Munch, J., Lazarow, K., Lutter, D., Mah, N., Andrade-Navarro, M. A., von Kries, J. P., Stauber, T., & Jentsch, T.J. (2014). Identification of LRRC8 heteromers as an essential component of the volume-regulated anion channel VRAC. *Science*, **344**(6184), 634–638.

Wang, L., Cao, L., Li, Z., Shao, Z., Chen, X., Huang, Z., He, X., Zheng, J., Liu, L., Jia, X. M., & Xiao, H. (2024). ATP-elicited cation fluxes promote volume-regulated anion channel LRRC8/VRAC transport cGAMP for antitumor immunity. *Journal of Immunology*, **213**(3), 347–361.

Wang, Y., Sun, Z., Ping, J., Tang, J., He, B., Chang, T., Zhou, Q., Yuan, S., Tang, Z., Li, X., Lu, Y., He, R., He, X., Liu, Z., Yin, L., & Wu, N. (2023). Cell volume controlled by LRRC8A-formed volume-regulated anion channels fine-tunes T cell activation and function. *Nature Communications*, **14**(1), 7075.

Widmer, C. A., Klebic, I., Domanitskaya, N., Decollogny, M., Howald, D., Siffert, M., Essers, P., Nowicka, Z., Stokar-Regenscheit, N., van de Ven, M., de Korte-Grimmerink, R., Galvan, J. A., Pritchard, C. E. J., Huijbers, I. J., Fendler, W., Vens, C., & Rottenberg, S. (2022). Loss of the volume-regulated anion channel components LRRC8A and LRRC8D limits platinum drug efficacy. *Cancer Research Communications*, **2**(10), 1266–1281.

Williams, J. O., Roche, T. E., & McFadden, B. A. (1971). Mechanism of action of isocitrate lyase from *Pseudomonas indigofera*. *Biochemistry*, **10**(8), 1384–1390.

Wittig, I., Beckhaus, T., Wumaier, Z., Karas, M., & Schagger, H. (2010). Mass estimation of native proteins by blue native electrophoresis: Principles and practical hints. *Molecular & Cellular Proteomics*, **9**(10), 2149–2161.

Woo, S. R., Fuertes, M. B., Corrales, L., Spranger, S., Furdyna, M. J., Leung, M. Y., Duggan, R., Wang, Y., Barber, G. N., Fitzgerald, K. A., Alegre, M. L., & Gajewski, T. F. (2014). STING-dependent cytosolic DNA sensing mediates innate immune recognition of immunogenic tumors. *Immunity*, **41**(5), 830–842.

Wu, J., Chen, Y. J., Dobbs, N., Sakai, T., Liou, J., Miner, J. J., & Yan, N. (2019). STING-mediated disruption of calcium homeostasis chronically activates ER stress and primes T cell death. *Journal of Experimental Medicine*, **216**(4), 867–883.

Wu, J., Dobbs, N., Yang, K., & Yan, N. (2020). Interferon-independent activities of mammalian STING mediate antiviral response and tumor immune evasion. *Immunity*, **53**(1), 115–126 e115.

Wu, X., Yi, X., Zhao, B., Zhi, Y., Xu, Z., Cao, Y., Cao, X., Pang, J., Yung, K. K. L., Zhang, S., Liu, S., & Zhou, P. (2023). The volume regulated anion channel VRAC regulates NLRP3 inflammasome by modulating itaconate efflux and mitochondria function. *Pharmacological Research*, **198**, 107016.

Yamada, T., Figueroa, E. E., Denton, J. S., & Strange, K. (2021). LRRC8A homohexameric channels poorly recapitulate VRAC regulation and pharmacology. *American Journal of Physiology-Cell Physiology*, **320**(3), C293–C303.

Yamada, T., & Strange, K. (2018). Intracellular and extracellular loops of LRRC8 are essential for volume-regulated anion channel function. *Journal of General Physiology*, **150**(7), 1003–1015.

Yamada, T., Wondergem, R., Morrison, R., Yin, V. P., & Strange, K. (2016). Leucine-rich repeat containing protein LRRC8A is essential for swelling-activated $Cl^-$ currents and embryonic development in zebrafish. *Physiological Reports*, **4**(19), e12940.

Zhang, J., & Lieberman, M. (1996). Chloride conductance is activated by membrane distention of cultured chick heart cells. *Cardiovascular Research*, **32**(1), 168–179.

Zhang, Y., Xie, L., Gunasekar, S. K., Tong, D., Mishra, A., Gibson, W. J., Wang, C., Fidler, T., Marthaler, B., Klingelhutz, A., Abel, E. D., Samuel, I., Smith, J. K., Cao, L., & Sah, R. (2017). SWELL1 is a regulator of adipocyte size, insulin signalling and glucose homeostasis. *Nature Cell Biology*, **19**(5), 504–517.

Zhao, H., Teng, D., Yang, L., Xu, X., Chen, J., Jiang, T., Feng, A. Y., Zhang, Y., Frederick, D. T., Gu, L., Cai, L., Asara, J. M., Pasca di Magliano, M., Boland, G. M., Flaherty, K. T., Swanson, K. D., Liu, D., Rabinowitz, J. D., & Zheng, B. (2022). Myeloid-derived itaconate suppresses cytotoxic $CD8^+$ T cells and promotes tumour growth. *Nature Metabolism*, **4**(12), 1660–1673.

Zheng, D., Liwinski, T., & Elinav, E. (2020). Inflammasome activation and regulation: Toward a better understanding of complex mechanisms. *Cell Discovery*, **6**, 36.

Zholos, A., Beck, B., Sydorenko, V., Lemonnier, L., Bordat, P., Prevarskaya, N., & Skryma, R. (2005). $Ca^{2+}$ — and volume-sensitive chloride currents are differentially regulated by agonists and store-operated $Ca^{2+}$ entry. *Journal of General Physiology*, **125**(2), 197–211.

Zhou, C., Chen, X., Planells-Cases, R., Chu, J., Wang, L., Cao, L., Li, Z., Lopez-Cayuqueo, K. I., Xie, Y., Ye, S., Wang, X., Ullrich, F., Ma, S., Fang, Y., Zhang, X., Qian, Z., Liang, X., Cai, S. Q., Jiang, Z., Zhou, D., Leng, Q., Xiao, T. S., Lan, K., Yang, J., Li, H., Peng, C., Qiu, Z., Jentsch, T. J., & Xiao, H. (2020). Transfer of cGAMP into bystander cells via LRRC8 volume-regulated anion channels augments STING-mediated interferon responses and anti-viral immunity. *Immunity*, **52**(5), 767–781 e766.

Zhou, P., Polovitskaya, M. M., & Jentsch, T. J. (2018). LRRC8 N termini influence pore properties and gating of volume-regulated anion channels (VRACs). *Journal of Biological Chemistry*, **293**(35), 13440–13451.

Zhou, Y., Fei, M., Zhang, G., Liang, W. C., Lin, W., Wu, Y., Piskol, R., Ridgway, J., McNamara, E., Huang, H., Zhang, J., Oh, J., Patel, J. M., Jakubiak, D., Lau, J., Blackwood, B., Bravo, D. D., Shi, Y., Wang, J., Hu, H. M., Lee, W. P., Jesudason, R., Sangaraju, D., Modrusan, Z., Anderson, K. R., Warming, S., Roose-Girma, M., & Yan, M. (2020). Blockade of the phagocytic receptor MerTK on tumor-associated macrophages enhances P2×7R-dependent STING activation by tumor-derived cGAMP. *Immunity*, **52**(2), 357–373 e359.

Zuccolini, P., Ferrera, L., Remigante, A., Picco, C., Barbieri, R., Bertelli, S., Moran, O., Gavazzo, P., & Pusch, M. (2022). The VRAC blocker DCPIB directly gates the BK channels and increases intracellular $Ca^{2+}$ in melanoma and pancreatic duct adenocarcinoma cell lines. *British Journal of Pharmacology*, **179**(13), 3452–3469.

## Additional information

### Competing interests

The authors declare no conflict of interest.

### Author contributions

S.Y., A.Z., F.A., A.A.C., S.T.G., J.Z. and A.R.C. drafted the manuscript; J.G. collected and analysed data from the PDB; S.Y., J.G. and A.R.C. interpreted the results. S.Y., A.Z., J.G., R.S., Y.R. and A.R.C. prepared the final version of the paper. All authors have read and approved the final version of the manuscript submitted for publication and agree to be accountable for all aspects of the work in ensuring that questions related to the accuracy or integrity of any part of the work are appropriately investigated and resolved. All persons designated as authors qualify for authorship, and all those who qualified are listed.

### Funding

This work was supported by the National Institutes of General Medical Sciences (NIGMS) of the National Institutes of Health (NIH) grant R35GM155189 to A.R.C. S.Y. was supported by a fellowship from the BioLAB Program. J.G. was supported by the Quad Faculty Research Grant Program from the College Centre for Research and Fellowships at the University of Chicago. F.A. and R.S. were supported by fellowships from the Biological Sciences Collegiate Division Research Endowments at the University of Chicago. A.R.C. acknowledges support from the Neubauer Family Foundation as well as the Cancer Research Foundation, the University of Chicago Medicine Comprehensive Cancer Centre (UCCCC) and the American Cancer Society Institutional Research Grant (ACS-IRG), and seed funding from the University of Chicago Centre for Inter-disciplinary Study of Inflammatory Intestinal Disorders (C-IID; P30 DK42086).

### Acknowledgements

We thank Francisco Bezanilla (UChicago), Xiaowei Hou (UC Cincinnati) and Navid Bavi (UCLA) for critical reading of the manuscript, and Eduardo Perozo (UChicago) and Marcos Sotomayor (UChicago) for helpful discussions.

### Keywords

immunotherapy, LRRC8, macrophages, structure–function, T cells, VRAC

## Supporting information

Additional supporting information can be found online in the Supporting Information section at the end of the HTML view of the article. Supporting information files available:

**Peer Review History**